Benzodithiophene Based Organic Dyes for DSSC: Effect of Alkyl Chain Substitution on Dye Efficiency

Clara Baldoli,[a*] Stefania Bertuolo,[b] Emanuela Licandro,[b] Lucia Viglianti,[b] Patrizia Mussini,[b] Gabriele Marotta,[c] Paolo Salvatori,[c, d] Filippo De Angelis,[c] Paola Manca,[e] Norberto Manfredi,[e] Alessandro Abbotto[e*]

[a]CNR - Istituto di Scienze e Tecnologie Molecolari. Via C. Golgi, 19. I-20133 Milano, Italy

[b] Dipartimento di Chimica. Università degli Studi di Milano. Via C. Golgi, 19. I-20133 Milano, Italy

[c]CNR - Istituto di Scienze e Tecnologie Molecolari. Computational Laboratory for Hybrid Organic Photovoltaics (CLHYO), via Elce di Sotto 8. I-06123 Perugia, Italy

[d] D3-Computation, Istituto Italiano di Tecnologia, Via Morego 30, I-16163 Genova, Italy

[e]Dipartimento di Scienze dei Materiali and Solar Energy Research Center MIB-SOLAR; INSTM Milano-Bicocca Unit, Università di Milano-Bicocca, Via Cozzi 55, I-20125, Milano, Italy

Abstract: A series of push-pull triarylamine organic dyes containing the benzo[1,2-*b*:4,5-*b*']dithiophene unit as a spacer and bearing alkyl chains in different positions of the molecule were synthesized. The new dyes **1-4** were characterized by optical and electrochemical measurements and density functional theory calculations and used as sensitizers in liquid dye-sensitized solar cells. The effect of alkyl chain position on dye properties and performances was investigated and dye **1**, bearing two 3,7-dimethyloctyl groups on the benzodithiophene core, exhibited the best behavior in term of light absorption and cell performance (PCE of 6.6%, to be compared with a PCE of 8.1% for N719-based device). The efficiency of the DSSC was highly dependent on the solvent used for the dye-sensitizing bath, which affects the position of the COOH/COO⁻ equilibrium.

Keywords

Push-pull dyes

Dye sensitized solar cells

Benzodithiophene

DFT-TDDFT

Cyclic voltammetry

Corresponding authors: Clara Baldoli. CNR - Istituto di Scienze e Tecnologie Molecolari. Via C. Golgi,19. I-20133 Milano, Italy. E-mail: clara.baldoli@istm.cnr.it. Tel.: +39 0250314143. Fax: +39 0250314139.

Alessandro Abbotto - Dipartimento di Scienze dei Materiali and Solar Energy Research Center MIB-SOLAR; INSTM. Milano-Bicocca Unit, Università di Milano-Bicocca, Via Cozzi 55, I-20125, Milano, Italy. E-mail: alessandro.abbotto@unimib.it. Tel.: +39 02 6448 5227. Fax: (+39) 02 6448 5400.

Introduction

In recent years metal-free organic dyes for DSSC [1,2,3,4] have been the object of a growing interest by organic chemists, because a great number of diverse structures can be easily prepared using well established synthetic methodologies and, through appropriate molecular design, their optical, electronic and electrochemical properties can be finely modulated.[5,6,7] The most efficient metal-free dyes for DSSC are characterized by a push-pull structure in which an electron-rich donor group communicates with an electron-acceptor one through a π-conjugated system which, not only determines cell light absorption regions, but also affects the electron injection from the dye excited state to the TiO_2 surface. A number of conjugated aromatic and heteroaromatic systems have been investigated as spacers and dyes containing substituted thiophene or thienothiophene bridges have already shown remarkable efficiencies when employed in DSSC. [2] On the contrary benzodithiophene systems, which own structural and electronic properties that match the π-spacer requests, have been widely employed in photovoltaic polymers[8] but less used in DSSC dye

[1][] Bong-Gi K., Kyeongwoon C. Jinsang K. Molecular Design Principle of All-organic Dyes for Dye-Sensitized Solar Cells. Chem. Eur. J. 2013; 19: 5220–5230.

[2][] Liang M., Chen J. Arylamine Organic Dyes for Dye-Sensitized Solar Cells *Chem. Soc. Rev.*; 2013, *42*: 3453-3488.

[3][] Kanaparthi, R. K., Kandhadi, J., Giribabu, Lingamallu. Metal-free organic dyes for dye-sensitized solar cells: recent advances *Tetrahedron*; 2012, 68(40): 8383-8393.

[4][] Ooyama, Y, Harima, Y. Photophysical and Electrochemical Properties, and Molecular Structures of Organic Dyes for Dye-Sensitized Solar Cells *Chem.Phys. Chem*. 2012**;** 13 (18): 4032-4080.

[5][] Amaresh, M, Markus, K, Fischer, R, Bäuerle P. Metal-free organic dyes for dye-sensitized solar cells: from structure: property relationships to design rules *Angew.Chem.Int. Ed.* 2009; 48: 2474-2499.

[6][] Pastore M.; Mosconi E.; Fantacci S., De Angelis F. Computational investigations on organic sensitizers for dye-sensitized solar cells *Curr. Org. Synth.* 2012; 9(2): 215-232.

[7][] Hara K., Molecular design of sensitizers for dye-sensitized solar cells. In Springer Series in Materials Science; Molecular Catalysts for Energy Conversion. 2009,111 p. 217-250.

[8][] Long Y., Shaoqing Z., Lijun H.,† Maojie Z., Jianhui H. Molecular Design toward Highly Efficient Photovoltaic Polymers Based on Two-Dimensional Conjugated Benzodithiophene *Acc. Chem. Res.* 2014; 47: 1595–1603.

structures. [9,10,11,12] We have already reported some preliminary results about the synthesis,

spectro-electrochemical characterization and cell efficiency of two new organic dyes (**CR52** and

CR29, figure 1) containing, respectively, the benzo[1,2-b:4,3-b']dithiophene (BDT) and the

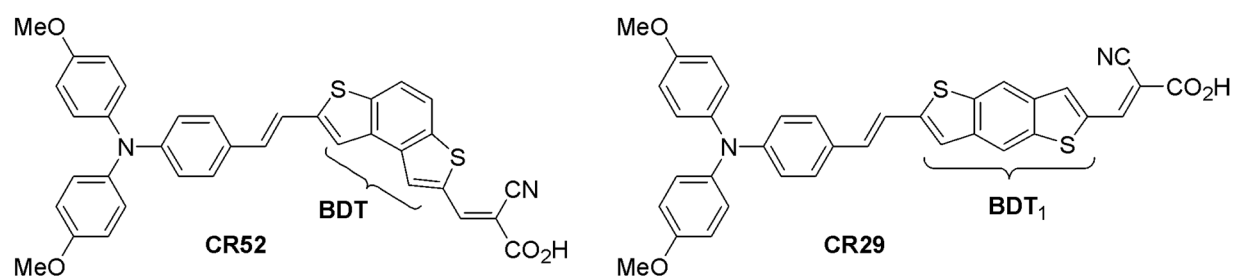benzo[1,2-b:4,5-b']dithiophene (BDT_1) as π-conjugated spacers. [13]

Figure 1. Structures of dyes **CR52** and **CR29**

In our previous work [13] we found out that dye **CR29** showed a better efficiency in DSSC tests

with respect to **CR52**. On the basis of DFT calculations, photophysical and cyclovoltammetric

characterization, this was attributed to the better conjugation of BDT_1 spacer, which results in a

more efficient communication between the triarylamine donor unit and the cyanoacetic acceptor

group. In a development of this work and with the aim of identifying more efficient dyes, with

improved performance with respect to **CR29**, we designed modified structures in which bulky alkyl

[9] Gao Y-R., Chu L.-L., Guo W., MaT.-L. Synthesis and photoelectric properties of an organic dye containing benzo[1,2-b:4,5-b0]dithiophene for dye-sensitized solar cells *Chin. Chem. Lett.* 2013; 24: 149-152.

[10] Gao P., Tsao H. N., Grätzel M., Nazeeruddin M. K Fine-tuning the Electronic Structure of Organic Dyes for Dye-Sensitized Solar Cells *Org. Lett*. 2012; 14: 4330–4333.

[11] Lin Y-Z. , Yeh C.-W., Chou P.-T., Watanabe M., Chang Y.-H. Chang Y. J., Chow T. J. Benzo[1,2-b:4,5-b']dithiophene and benzo[1,2-b:4,5-b']difuran based organic dipolar compounds for sensitized solar cells *Dyes and Pigm.* 2014; 109: 81-89.

[12] Hao X., Liang M., Cheng X., Pian X., Sun Z., Xue S., Organic Dyes Incorporating the Benzo[1,2-b:4,5-b′]dithiophene Moiety for Efficient Dye-Sensitized Solar Cells *Org. Lett*. 2011; 13: 5424–5427.

[13] Longhi E., Bossi A., Di Carlo G., Maiorana S., De Angelis F. , Salvatori P., Petrozza A., Binda M., Roiati V., Mussini P. R., Baldoli C., Licandro E.Metal-Free Benzodithiophene-Containing Organic Dyes for Dye-Sensitized Solar Cells *Eur. J. Org. Chem.* 2013, 84–94.

chains were inserted in different positions of the molecule. In fact, it is well known that some

detrimental processes such as dye aggregation at TiO_2 surface and enhanced charge recombination

at the TiO_2/electrolyte interface can be successfully reduced by introducing alkyl chains on the

donor [14] or π-linker.[15,16] We therefore synthesized the series of dyes **1-4**, (Figure 2) derived from

the parent **CR29**, in which a 3,7-dimethyloctyl- and/or cyclohexylethyl chain is present on

triarylamine or benzodithiophene unit, and also investigated the structure/performance correlation
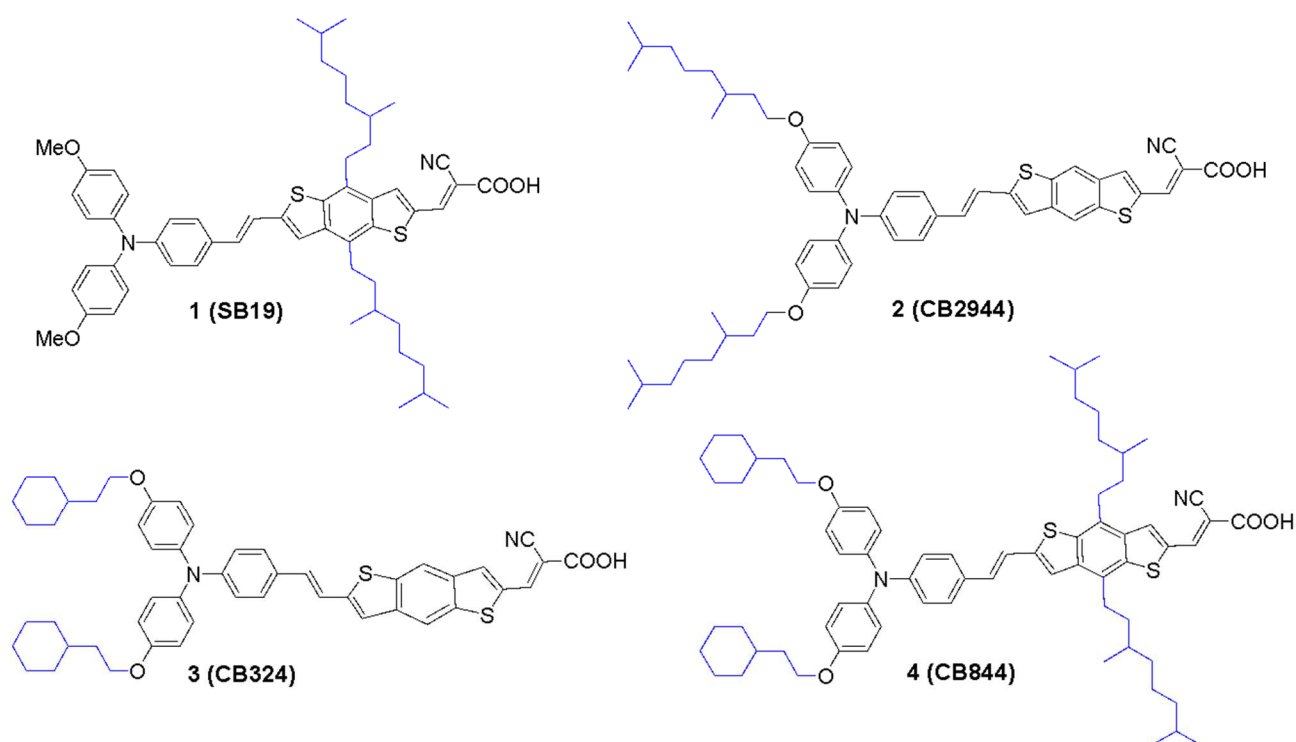
in such dyes.

Figure 2. **BDT₁** based dyes **1-4**

[14] Yu Q-Y,. Liao J-Y,. Zhou S-M, Shen Y., Liu J-M., Kuang D-B., Su C-Y. Effect of hydrocarbon chain length of disubstituted triphenyl-amine-based organic dyes on dye-sensitized solar cells *J. Phys. Chem. C* 2011; 115: 22002–22008.

[15] Wang X., Guo L., Xia P.F., Zheng F., Wong M.S., Zhu Z. Dye-sensitized solar cells based on organic dyes with naphtho[2,1-b:3,4-b0]dithiophene as the conjugated linker. *J Mater Chem A* 2013;1:13328-13336

[16] Koumura N., Wang Z.-S., Mori S., Miyashita M., Suzuki E., Hara K. Alkyl functionalized organic dyes for efficient molecular photovoltaics. *J. Am. Chem. Soc*. 2006;128: 14256-14257.

2. Material and methods

2.1. Reagents

All reagents and solvents were obtained from highest grade commercial sources and used without further purification unless otherwise stated. Benzo[1,2-b:4,5-b']dithiophene-4,8-dione **15** is a commercially available compound. Dye samples for cell fabrication were checked by HPLC analysis and the purity was estimated to be over 98%. Compounds **CR29**, **5a**, **6d**, **11**, have been synthesized as previously reported. [13,17]

2.2. Computational details

All calculations were carried out with the Gaussian09 program package. [18] Geometry optimization of the stand-alone dye molecules was made by using the B3LYP hybrid functional [19] and 6-31G* basis set [20] in vacuo. Geometry optimization was followed by excited state TD-DFT calculations in order to simulate the UV-Vis absorption spectra with the MPW1K exchange-correlation [21] and a 6-31G* basis set, both in gas phase and in ACN solution. The effect of the solution was included

[17][] Faccini M., Balakrishnan M., Diemeer M. B., Hu Z.-P., Clays K., Asselberghs I., Leinse A., Driessen A., Reinhoudt D. N., Verboom W., Enhanced poling efficiency in highly thermal and photostable nonlinear optical chromophores *J. Mater. Chem.* 2008, 18: 2141–2149.

[18][] Frisch, M. J.; Trucks, G. W.; Schlegel, H. B.; Scuseria, G. E.; Robb, M. A.; Cheeseman, J. R.; Montgomery, J. A. J.; Vreven, T.; Kudin, K. N.; Burant, J. C.; Millam, J. M.; Iyengar, S. S.; Tomasi, J.; Barone, V.; Mennucci, B.; Cossi, M.; Scalmani, G.; Rega, N.; Petersson, G. A.; Nakatsuji, H.; Hada, M.; Ehara, M.; Toyota, K.; Fukuda, R.; Hasegawa, J.; Ishida, M.; Nakajima, T.; Honda, Y.; Kitao, O.; Nakai, H.; Klene, M.; Li, X.; Knox, J. E.; Hratchian, H. P.; Cross, J. B.; Bakken, V.; Adamo, C.; Jaramillo, J.; Gomperts, R.; Stratmann, R. E.; Yazyev, O.; Austin, A. J.; Cammi, R.; Pomelli, C.; Ochterski, J. W.; Ayala, P. Y.; Morokuma, K.; Voth, G. A.; Salvador, P.; Dannenberg, J. J.; Zakrzewski, V. G.; Dapprich, S.; Daniels, A. D.; Strain, M. C.; Farkas, O.; Malick, D. K.; Rabuck, A. D.; Raghavachari, K.; Foresman, J. B.; Ortiz, J. V.; Cui, Q.; Baboul, A. G.; Clifford, S.; Cioslowski, J.; Stefanov, B. B.; Liu, G.; Liashenko, A.; Piskorz, P.; Komaromi, I.; Martin, R. L.; Fox, D. J.; Keith, T.; Al-Laham, M. A.; Peng, C. Y.; Nanayakkara, A.; Challacombe, M.; Gill, P. M. W.; Johnson, B.; Chen, W.; Wong, M. W.; Gonzalez, C.; Pople, J. A. Gaussian, Inc., Wallingford CT, 2009.

[19][] Becke, A. D. Density functional thermochemistry. III. The role of exact exchange *J.Chem. Phys.* 1993, 98: 5648-5652.

[20][] Binkley, J. S.; Pople, J. A.; Hehre, W. J. Self-consistent molecular orbital methods. 21. Small split-valence basis sets for first-row elements *J. Am. Chem. Soc.* 1980, 102: 939-947.

[21][] Lynch, B. J.; Fast, P. L.; Harris, M.; Truhlar, D. G. Adiabatic Connection for Kinetics *J. Phys. Chem. A*. 2000, 104: 4811-4815.

using the polarizable continuum model of solvation (CPCM). [22] The molecular orbitals energy levels and isodensity plot have been extrapolated by a single point calculation (B3LYP/6-31G*) in solution. This computational approach was demonstrated to be reliable for the description of optoelectronic properties of similar Donor-π-Acceptor [23] sensitizers.

2.3. Electrochemistry

The molecules have been characterized by cyclic voltammetry at potential scan rates typically ranging from 0.05 to 2 V s^{-1}, performed by an AUTOLAB PGSTAT potentiostat of EcoChemie (Utrecht, The Netherlands) run by a PC with the GPES software of the same manufacturer. The molecules were investigated at ~0.0005 M concentration in CH_2Cl_2 + 0.1 M TBAP, in a 4 cm^3 minicell, deaerated by N_2 purging.

Additional general experimental details are reported in supporting information.

2.4. Synthetic procedures

4-[bis[4-(3,7-dimethyloctyloxy)phenyl]amino]phenyl]methyl]triphenyl phosphonium bromide (5b): a solution of **14b** (0.56 mmol) and PPh$_3$·HBr (0.7 g, 0.67 mmol) in CHCl$_3$ (6 mL) was refluxed under stirring for 4 h. The solvent was then evaporated and the residue was treated with diisopropylether (3 mL) and stirred to obtain a dusty pale yellow solid in 75 % yield, ^{1}H-NMR (300MHz, CDCl$_3$): δ, ppm = 0.83-0.85 (d, 12H, *J*= 6.6 Hz); 0.89-0.92 (d, 6H, *J*=6.4 Hz); 1.09-1.32(m, 12H); 1.48-1.57 (m, 2H); 1.70-1.77 (m, 2H), 3.89-3.94 (m, 4H); 5.12-5.17 (d, 2H, *J*$_{H-P}$=13.3); 6.59-6.62 (d, 2H, *J*=7.9); 6.74-6.78 (m, 6 H); 6.91-6.94 (d, 4H, *J*=8.7); 7.43-7.73 (m, 15H). ^{13}C-NMR (75 MHz, CDCl$_3$): 19.55, 22.48, 22.57, 24.50, 27.82, 29.73, 30.37, 30.98, 36.16, 37.17, 39.11, 66.50, 115.09, 116.91, 117.02, 117.42, 118.55, 119.67, 121.20, 125.91, 128.37, 128.80,

[22] Cossi, M.; Rega, N.; Scalmani, G.; Barone, V. Energies, structures, and electronic properties of molecules in solution with the C-PCM solvation model *J. Comput. Chem.* 2003, 24: 669-681.

[23] Pastore, M.; Mosconi, E.; De Angelis, F.; Graetzel, M. A Computational Investigation of Organic Dyes for Dye-Sensitized Solar Cells: Benchmark, Strategies, and Open Issues *J. Phys. Chem. C* 2010, 114: 7205 – 7212.

128.90, 130.02 130.18, 131.85, 131.92, 132.07, 133.59, 133.82, 134.29, 134.42, 134.87, 139.91, 148.90, 155.65. ^{31}P-NMR (121 MHz, CDCl$_3$): δ, ppm = 22.98.

4-[bis[4-(2-cyclohexylethoxy)phenyl]amino]phenyl]methyl]triphenyl phosphonium bromide (5c): it was obtained with the same procedure for **5b,** starting from alcohol **14c**, as yellowish solid (76%). ^{1}H-NMR (300 MHz, DMSO): δ, ppm =0.85-1.03 (m, 4H); 1.07-1.19 (m, 6H); 1.25-1.41 (m, 2H); 1.53-1.70 (m, 14H); 3.91 (t, 4H, J= 6.4 Hz); 4.97 (d, 2H, J_{H-P}=14.6); 6.49-6.51 (d, 2H, J= 8.1); 6.68-6.71 (d, 2H, J= 8.3); 6.83-6.93 (m, 4H); 7.50-7.70 (m, 15H); 7.83-7.88 (m, 4H). ^{13}C-NMR (75 MHz, DMSO): δ, ppm =25.65, 25.84, 25.98, 27.26, 27.87, 32.63, 33.95, 36.05, 65.57, 115.42, 115.69, 117.39, 117.85, 117.96, 118.52, 118.87, 126.65, 128.58, 128.73, 129.88, 130.05, 131.33, 131.40, 131.92, 133.90, 134.03, 134.92, 139.44, 148.39, 148.43, 155.31. ^{31}P-NMR (121 MHz, DMSO): δ, ppm = 23.52.

4,8-bis(3,7-dimethyloctyl)benzo[1,2-*b*:4,5-b']dithiophene-2,6-dicarbaldehyde (6e): a solution of *n*BuLi (1.6 M in hexane, 0.9 mL, 1.44 mmol) was added at -78°C to a solution of **16** (0.15 g, 0.33 mmol) in dry THF (3 mL), the white suspension thus formed was stirred at -78°C for 90 min. Dry DMF (0.5 mL) was added dropwise and the light yellow suspension was stirred at the same temperature for 2.5 h. The solvent was evaporated, the residue treated with 0.1 M solution of HCl (5mL) and extracted with CH$_2$Cl$_2$ (4x15 mL). The organic phase was washed with H$_2$O (15mL), dried over Na$_2$SO$_4$, filtered and the solvent evaporated. The crude product was purified by column chromatography (eluent: hexane/CH$_2$Cl$_2$, 7:3) to give **6e** as a yellow solid in 80% yield. M.p. 108-110 °C. IR (Nujol, cm^{-1}): 1685 (v CO). ^{1}H-NMR (300 MHz, CDCl$_3$): δ, ppm = 0.86-0.88 (d, 12H, J= 6.6 Hz), 1.06-1.08 (d, 6H, J=6.4 Hz), 1.15-1.28 (m, 12H), 1.51-1.61 (m, 6H), 1.63-1.64 (m, 2H), 3.20-3.22 (m, 4H), 8.17 (s, 2H), 10.17 (s, 2H). ^{13}C-NMR (75 MHz, CDCl$_3$):δ, ppm = 19.63, 22.63, 22.71, 24.74, 27.99, 30.88, 33.29, 36.96, 37.04, 39.28, 132.27, 133.47, 137.56, 139.68, 144.40, 184.62. HRSM (EI) (m/z): HRMS-EI (m/z): found [M]+ 526.2890; molecular formula C$_{32}$H$_{46}$O$_2$S$_2$

requires 526.2839. UV-vis CH_2Cl_2 (6.83E-05 M): λmax = 351 nm (ε = 4.01E+04 M^{-1} cm^{-1}), 445 nm (ε = 1.19E+04 M^{-1} cm^{-1}).

***E*-6-{4-[Bis(4-methoxyphenyl)amino]phenyl}ethenyl)-4,8-bis(3,7-dimethyloctyl)benzo[1,2-b:4,5-b']dithiophen-2-carbaldehyde (7) :** a solution of **5a** [13] (65 mg, 0.09 mmol) in DMF (3 mL) was slowly added at room temperature to a slurry of 4,8-bis(3,7-dimethyloctyl)benzo[1,2-b:4,5-b']dithiophene-2,6-dicarbaldehyde (**6e**) (60 mg, 0.11 mmol), 18-crown-6 ether (10 mg), and anhydrous K_2CO_3 (30 mg, 0.2 mmol) in DMF (2.5 mL). The resulting orange solution was stirred 24h at room temperature. The solution was then poured into brine (10 mL) and extracted with CH_2Cl_2 (4x10 mL). The organic phase was washed with water (10 mL), dried with Na_2SO_4 and filtered. After evaporation of the solvent, the crude dark-orange product was purified by silica gel column chromatography (hexane/AcOEt, 10:1.5) to give **1** as a red solid in 84 % yield.

M.p. 58-61 °C. IR (Nujol, cm^{-1}): 1698 (ν CO). ^{1}H-NMR (300 MHz, $CDCl_3$): δ, ppm = 0.90-0.91 (d, 6H, *J*=6.6 Hz); 0.92-0.93 (d, 6H, *J*=6.6 Hz); 1.07-1.09 (d, 3H, *J*=6.2 Hz); 1.10-1.12 (d, 3H, *J*=6.2 Hz); 1.19-1.44 (m, 12H), 1.56-1.65 (m, 6H), 1.76-1.85 (m, 2H), 3.07-3.19 (m, 4H); 3.84 (s, 6H); 6.86-6.90(m, 4H); 6.92-6.94 (d, 2H, *J*= 8.8 Hz); 6.98-7.03 (d, 1H, *J*=15.9 Hz); 7.09-7.13 (m, 4H); 7.19-7.25 (d, 1H, *J*=15.9 Hz); 7.29 (s, 1H); 7.34-7.36 (d, 2H, *J*=8.8 Hz); 8.13 (s, 1H), 10.12 (s, 1H). ^{13}C-NMR (75 MHz, $CDCl_3$): δ, ppm = 19.64 19.72, 22.64, 22.71, 24.71, 27.97, 28.02, 30.70, 30.85, 33.24, 36.44, 36.89, 36.96, 39.32, 55.46, 114.76, 119.34, 119.76, 120.09, 126.96, 127.55, 128.16, 129.17, 132.04, 132.15, 132.96, 134.81, 136.61, 139.83, 140.33, 141.98, 145.69, 149.03, 156.23, 184.48. HRMS-EI (m/z): found $[M]^+$ 827.4459; molecular formula $C_{53}H_{65}NO_3S_2$: requires 827.4406. UV-vis CH_2Cl_2 (3.38E-05 M): λ_{max} = 461 nm (ε=6.47E+04 M^{-1} cm^{-1}).

***E*-6-{4-[Bis(3,7-dimethyloctyloxy)amino]phenyl}ethenyl)benzo[1,2-b:4,5-b']dithiophen-2-carbaldehyde (8):** it was obtained, following the same procedure for **7**; the crude product was purified by silica gel column chromatography (CH_2Cl_2) to give **8** as a red-orange solid in 63% yield.

M.p. 89-92 °C. IR (Nujol, cm^{-1}): 1698 (ν CO). ^{1}H-NMR(300MHz, $CDCl_3$): δ, ppm = 0.87-0.89 (d, 12H, *J*= 6.6 Hz); 0.95-0.97 (d, 6H, *J*=6.4 Hz); 1.14-1.37 (m, 12H); 1.53-1.68 (m, 6H); 1.80-1.85

(m, 2H); 3.98-4.01 (m, 4H); 6.83-6.89 (m, 6H); 6.93-6.98 (d, 1H, J=15.9); 7.04-7.21 (m, 6H); 7.30-7.33 (d, 2H, J= 8.4); 7.99 (s, 1H);8.10 (s, 1H); 8.25 (s,1H); 10.08 (s, 1H, CHO). ^{13}C-NMR (75 MHz, CDCl$_3$): 19.55, 19.68, 19.81, 22.60, 22.69, 24.65, 27.97, 29.69, 29.75, 29.88, 36.11, 36.18, 36.30, 37.12, 37.31, 37.44, 39.26, 39.39, 66.61, 66.80, 115.34, 116.67, 118.95, 119.31, 119.73, 120.92, 127.04, 127.56, 132.69, 133.97, 135.98, 136.97, 139.55, 141.54, 143.18, 147.05, 155.96, 184.34. HRMS-EI (m/z): found [M]$^+$ 799.4087; molecular formula C$_{51}$H$_{61}$NO$_3$S$_2$: requires 799.4092. UV-vis CH$_2$Cl$_2$ (2.82E-05 M): λmax = 453 nm (ε = 5.51E+04 M^{-1} cm^{-1}).

6-(2-{4-[Bis(2-cyclohexylethoxy)amino]phenyl}ethenyl)benzo[1,2-b:4,5-b']dithiophen-2-carbaldehyde (9) : it was obtained, following the same procedure for **7**; the crude product was purified by silica gel column chromatography (CH$_2$Cl$_2$/hexane, 9:1) to give **9** as a red-orange solid in 60% yield. M.p. 161-163 °C. IR (Nujol, cm^{-1}): 1714 (ν CO).^{1}H-NMR (300 MHz, DMSO-d6) E isomer: δ, ppm =0.86-0.96 (m, 4H); 1.14-1.19 (m, 6H); 1.40-1.42 (m, 2H); 1.54-1.72 (m, 14H); 3.94 (t, 4H, J= 6.5); 6.67-6.70 (d, 2H, J= 8.5); 6.86-6.92 (m, 5H); 6.98-7.01 (m, 4H),7.36-7.38 (d, 1H, J=16.1 Hz); 7.40-7.42 (m, 3H); 8.39 (s, 2H); 8.59 (s, 1H); 10.09 (s, 1H). ^{13}C-NMR (75 MHz, DMSO): δ, ppm =25.68, 25.80, 25.87, 26.00, 32.65, 33.98, 36.07, 65.61, 115.47, 117.07, 118.33, 119.05, 120.09, 121.52, 127.07, 127.31, 127.90, 132.10, 135.61, 136.00, 136.09, 138.46, 139.30, 141.10, 142.59,146.38, 148.75, 155.54, 185.96. UV-vis CH$_2$Cl$_2$ (3.95 E-05 M): λ$_{max}$ = 453 nm (ε = 5.86E+04 M^{-1} cm^{-1}). HRMS-EI (m/z): found [M]$^+$ 739.3168; molecular formula C$_{47}$H$_{49}$NO$_3$S$_2$: requires 739.3153.

_E_-6-{4-[Bis(2-cyclohexylethoxy)amino]phenyl}ethenyl)-4,8-bis(3,7-dimethyloctyl)benzo[1,2-b:4,5-b']dithiophen-2-carbaldehyde (10): it was synthesized following the same procedure for **7**, by reaction of **5c** with aldehyde **6e**. Compound **10** was purified by column chromatography (eluent: CH$_2$Cl$_2$/hexane, 1:1) and isolated in 60% yield as a red solid. M.p. 169-170 °C (dec.). IR (Nujol, cm^{-1}): 1715 (ν CO). ^{1}H-NMR (300 MHz, CDCl3): δ, ppm = 0.86-0.92 (m, 12H), 1.01-1.10 (m, 12H), 1.19-1.22 (m, 12H), 1.26-172 (m, 28H), 2.98-3.23 (m, 4H), 3.97-3.99 (m, 4H), 6.82-7.37 (m, 15H), 8.09 (s, 1H), 10.09 (s, 1H) rifare in DMSO ^{13}C-NMR (75 MHz, CDCl$_3$): δ, ppm = 19.64,

19.73, 22.64, 22.71, 24.69, 24.71, 26.24, 26.44, 26.54, 27.98, 28.02, 30.69, 30.84, 33.25, 33.32, 34.55, 36.44, 36.73, 36.90, 36.97, 39.329, 66.22, 115.32, 119.26, 119.67, 120.00, 123.84, 126.98, 129.13, 132.00, 132.20, 132.86, 134.80, 136.62, 139.84, 140.06, 141.99, 143.13, 145.72, 155.87. HRSM (EI) (m/z): HRMS-EI (m/z): found $[M]^+$ 1019.6305; molecular formula $C_{67}H_{89}NO_3S_2$ requires 1019.6283. UV-vis CH_2Cl_2 (3.68E-05 M): λ_{max}= 460 nm (ε=5.49E+04 M^{-1} cm^{-1}).

2-Cyano-3-[6-(2-{4-{bis(4-methoxy)amino}phenyl}ethenyl)-4,8-bis(3,7-dimethyloctyl)benzo [1,2-b:4,5-b']dithiophen-2-yl]propenoic Acid (1): cyanoacetic acid (50.0 mg, 0.65 mmol) and piperidine (0.06 mmol) were added to a solution of **7** (90 mg, 0.1 mmol) in THF (4 mL). The reaction mixture was refluxed for 8 h. The solvent was then evaporated and the residue was taken up with a mixture of HCl 0.5M (6 mL) and hexane (3mL) then filtered washing the solid with aqueous MeOH. M.p. 192-193 °C (dec) ^{1}H-NMR (300 MHz, acetone d_6): δ, ppm = 0.87-0.90 (m, 12), 1.08-1.09 (m, 6H), 1.20-1.70 (m, 16H), 1.82-1.88 (m, 4H), 3.16 (m, 4H), 3.79 (s, 6H), 6.83-6.85(d, 2H, J=8.7 Hz), 6.94.6.97 (d, 4H, J=8.9 Hz), 7.05-7.11 (d, 1H, J=16.4 Hz), 7.12-7.14 (d, J=8.9 Hz, 4H), 7.42-7.49 (m, 3H), 7.55 (s, 1H), 8.40 (s, 1H), 8.54 (s, 1H). ^{13}C-NMR (75 MHz, DMSO d_6): δ, ppm = 19.50, 22.40, 24.00, 27.33, 32.31, 36.17, 43.64, 55.19, 114.98, 116.71, 118.30, 119.27, 120.70, 127.13, 127.42, 127.75, 128.13, 130.87, 131.63, 134.14, 134.89, 135.82, 139.06, 139.43, 145.06, 145.59, 148.67, 156.10, 163.07 UV-vis**:** CH_2Cl_2 (5.14E-05 M): λ_{max}= 517 nm (ε=3.42E+04 M^{-1} cm^{-1}), Maldi-TOF mass, found: 894.23; molecular formula $C_{56}H_{66}N_2O_4S_2$ requires: 894.44.

2-Cyano-3-[6-(2-{4-{bis(3,7-dimethyloctyl)amino}phenyl}ethenyl)-benzo[1,2-b:4,5-b']dithio phen-2-yl]propenoic Acid (2): it was obtained as dark red solid in 72% yield, following the same procedure of **1.** The crude product was purified by column chromatography (CH_2Cl_2/MeOH, 8:1). The residue was then treated with HCl 0.5M and filtered giving **2** as dark red solid**.** M.p.: 243-244 °C (dec.). ^{1}H-NMR (300 MHz, DMSO-d6): δ, ppm = 0.86-0.88 (d, 12H, J= 6.6 Hz), 0.92-0.94 (d, 6H, J=6.4 Hz), 1.14-1.40 (m, 12H), 1.48-1.79 (m, 8H), 4.01 (t, 4H, J=6.5 Hz), 6.75-6.78 (d, 2H, J= 8.5 Hz), 6.90-6.93 (d, 4H, J= 8.8 Hz), 6.94-6.99 (d, 1H, J= 15.5 Hz), 7.06-7.07 (d, 4H, J= 8.8 Hz),

7.32-7.37 (d, 1H, J= 15.5 Hz), 7.42-7.44(m, 3H), 8.02 (s, 1H), 8.26 (s, 1H), 8.36 (s, 1H), 8.41 (s, 1H). ^{13}C-NMR (75 MHz, DMSO):δ, ppm = 19.44, 20.57, 22.01, 22.42, 22.52, 23.06, 24.02, 27.32, 28.63, 28.94, 29.22, 35.64, 36.56, 65.96, 115.52, 116.47, 118.21, 118.45, 119.26, 121.72, 127.04, 127.48, 127.84, 135.70, 136.03, 136.95, 138.22, 139.37, 140.00, 145.53,148.66, 155.50, 162.76. Maldi-TOF mass, found 866.52; molecular formula $C_{54}H_{62}N_2O_4S_2$ requires 866.41.

2-Cyano-3-[6-(2-{4-{bis(2-cyclohexylethoxy)amino}phenyl}ethenyl)-benzo[1,2-b:4,5-b']dithio phen-2-yl]propenoic Acid (3): it was obtained as dark red solid in 74% yield, following the same procedure of **2**. M.p. 189-190 °C (dec.) ^{1}H-NMR (300 MHz, DMSO-d6): δ, ppm =0.89-0.93(m, 4H); 1.14-1.19 (m, 6H); 1.42-1.46 (m, 2H); 1.54-1.71 (m, 14H); 3.93 (t, 4H, J= 6.6 Hz); 6.67-6-70 (d, 2H, J= 8.6); 6.86-6.92 (m, 5H); 6.97-7.01 (m, 4H); 7.32-7.37 (d, 1H, J= 16.2 Hz); 7.38-7.41 (m, 3H); 7.93 (s, 1H); 8.18 (s, 1H); 8.33 (s, 2H). ^{13}C-NMR (75 MHz, CDCl$_3$): δ, ppm =25.67, 26.00, 28.86, 32.66, 33.98, 36.08, 38.67, 65.61, 115.46, 116.42, 117.99, 118.48, 119.27, 121.71, 126.99, 127.49, 127.80, 131.53, 135.78, 135.95, 137.22, 138.03, 139.35, 139.79, 141.00, 145.31, 148.61, 155.49, 162.64. Maldi-TOF mass found 806.61; molecular formula $C_{50}H_{50}N_2O_4S_2$ requires 806.32.

2-Cyano-3-[6-(2-{4-{bis(2-cyclohexylethoxy)amino}phenyl}ethenyl)-4,8-bis(3,7-dimethyloctyl) benzo [1,2-b:4,5-b']dithiophen-2-yl]propenoic Acid (4): it was obtained as purple solid in 70% yield, following the same procedure of **2**. M.p. 100-103 °C (dec.). ^{1}H-NMR (300 MHz, DMSO d6): δ, ppm = 0.77-0.83 (m, 16H), 0.85-0.98 (m, 10H), 1.09-1.71 (m, 42H), 2.92-3.04 (m, 4H), 3.91-3.95 (m, 4H), 6.69-6.72 (d, 2H, J= 8.6 Hz), 6.84-6.92 (m, 5H), 6.97-7.01 (d, J = 8.6 Hz 4H), 7.31-7.37 (m, 3H), 7.45 (s, 1H), 8.23 (s, 1H), 8.39 (s, 1H). ^{13}C-NMR (75 MHz, DMSO): δ, ppm = 19.53, 19.66, 22.66, 22.73, 24.69, 26.02, 26.26, 26.56, 27.98, 30.40, 30.75, 33.16, 33.35, 34.58, 36.77, 39.33, 66.21, 115.31, 119.96, 126.82, 127.06, 127.55,128.43, 140.27, 155.73. MS-Maldi-TOF mass (m/z) found: 1086.02; molecular formula$C_{70}H_{90}N_2O_4S_2$: requires 1086.6342.

***N,N*-bis-[4-(3,7-dimethyloctyloxy)phenyl]aniline (12b)**: to a solution of **11** (0.4 g, 1.4 mmol) in dry CH$_3$CN (8 mL), K$_2$CO$_3$ (0.5 g, 3.6 mmol) and 18-crown-6 (10 mg) were added and the mixture was stirred for 30 min.; 3,7-dimethyloctylbromide (0.7g, 3.3 mmol) was then added and the mixture

was heated to 80 °C under stirring for 20 h. The solvent was evaporated and the residue was taken-up with AcOEt (20 mL), filtered over a pad of celite and added with H_2O (30 mL). The aqueous phase was extracted with AcOEt (4x10 mL) dried over Na_2SO_4, and the solvent evaporated. The crude residue was purified by column chromatography (CH_2Cl_2) to give **12b** as thick pale yellow oil in 80 % yield. ^{1}H-NMR(300MHz, CDCl$_3$): δ, ppm= 0.89-0.96 (d, 12H, *J*= 6.6 Hz); 0.96-0.98 (d, 6H, *J*= 6.4 Hz) 1.15-1.28 (m, 6H); 1.29-1.38 (m, 6H), 1.54-1.60(m, 6H); 1.81-1.83 (m, 2H); 3.95-4.00 (m, 4H); 6.81-6.86 (m, 5H); 6.94-6.96 (d, 2H, *J*=8.0 Hz); 7.03-7.06 (d, 4H, J= 8.7Hz); 7.14-7.19 (m, 2H). ^{13}C-NMR(300MHz, CDCl$_3$): δ, ppm=19.69; 22.61; 22.70; 24.65; 27.96; 29.86; 36.33; 37.31; 39.26; 66.54; 115.24; 120.43; 120.85; 126.36; 128.85; 140.99; 148.85; 155.28. HRSM (EI)(m/z): [M]$^+$ found 557.4237; molecular formula $C_{38}H_{55}NO_2$ requires 557.4233.

***N,N*-bis-[4-(2-cyclohexylethoxy)phenyl]aniline (12c)**: it was obtained with the same procedure of **12b**. The crude residue treated with MeOH (5 mL) to give an off-white solid that was filtered: 530 mg (70%). M.p. 84-86 °C. ^{1}H-NMR (300 MHz, DMSO): δ, ppm =0.86-0.96 (m, 4H); 1.07-1.24 (m, 6H); 1.36-1.45 (m, 2H); 1.53-1.71 (m, 14H); 3.92 (t, 4H, *J*= 6.53); 6.78-6.81 (m, 5H); 6.91-6.95 (m, 2H), 7.01-7.04 (m, 4H), 7.13-7.18 (m, 2H). ^{13}C-NMR (75 MHz, DMSO): δ, ppm = 25.67, 25.80, 25.87, 26.00, 32.46, 32.52, 32.65, 32.78, 33.98, 36.09, 38.67, 38.94, 65.57, 114.76, 115.35, 119.71, 120.14, 126.31, 127.10, 128.97, 140.14, 148.39, 154.96. HRSM (EI) (m/z): [M]$^+$ found 497.3280; molecular formula $C_{34}H_{43}NO_2$ requires 497.3293.

4-[bis[4-(3,7-dimethyloctyloxy)phenyl]amino]benzaldehyde (13b): (Chloromethylene)dimethyl iminium chloride (0.31g, 2.4 mmol) was added to a solution of **12b** (0.6 mmol) in $(CH_2)_2Cl_2$ (8 mL) and the reaction mixture was heated at 80°C for 8 h, then a saturated NH_4Cl solution (10 mL) was added and the phases separated. The aqueous phase was extracted with AcOEt (4x10mL), the combined organic phases were dried over Na_2SO_4, and the solvent evaporated. The crude product was purified by column chromatography (eluent: CH_2Cl_2) to afford **13b** as yellow thick oil in 85 % yield. ^{1}H-NMR(300MHz, CDCl$_3$): δ, ppm = 0.88-0.90 (d, 12H, *J*= 6.6 Hz); 0.96-0.97 (d, 6H, *J*=6.4 Hz); 1.18-1.21 (m, 4H); 1.28-1.37 (m, 4H) 1.56-1.84 (m, 12H); 3.98 (t, 4H, J= 3.9); 6.83-6.89 (m,

6H); 7.09-7.12 (m, 4H); 7.60-7.63 (d, 2H, J= 8.6); 9.77 (s, 1H, CHO). ^{13}C-NMR (75 MHz, CDCl$_3$): δ, ppm = 19.60, 22.53, 22.63, 24.56, 27.87, 29.58.29.63, 29.77, 36.02, 36.15, 36.28, 37.07, 37.20, 39.16, 66.46, 115.33, 115.52, 115.71, 116.62, 127.68, 127.91, 128.10, 131.26, 138.54, 154.01, 156.84, 189.90. IR (neat): 1690 cm^{-1}(ν CO). HRSM (EI) (m/z): [M]$^+$ found 585.4172; molecular formula C$_{39}$H$_{55}$NO$_3$ requires 585.4182.

4- [bis[4-(2-cyclohexylethoxy)phenyl]amino]benzaldehyde (13c) CB281013: it was obtained following the same procedure for **13b**. The crude product was purified by column chromatography (eluent: CH$_2$Cl$_2$) to afford **13c** as a bright yellow thick oil, 0.27g (84% yield). ^{1}H-NMR(300MHz, CDCl$_3$): δ, ppm = 0.91-1.03 (m, 4H); 1.14-1.32 (m, 6H); 1.45-1.53 (m, 2H); 1.64-1.78 (m, 14H); 3.98 (t, 4H, J= 6.6 Hz); 6.82-6.89 (m, 6H); 7.08-7.13 (m, 4H); 7.59-7.62 (d, 2H, J= 8.7 Hz); 9.75 (s, 1H, CHO). ^{13}C-NMR (75 MHz, CDCl$_3$): δ, ppm = 26.23, 26.37, 26.52, 33.30, 34.54, 36.65, 66.23, 115.58, 116.70, 127.72, 128.01, 131.37, 138.61, 154.15, 156.94, 190.19. IR (neat): 1689 cm^{-1}(ν CO). HRSM (EI) (m/z): [M]$^+$ found 525.3245; molecular formula C$_{35}$H$_{43}$NO$_3$ requires 525.3243.

4-[bis[4-(3,7-dimethyloctyloxy)phenyl]amino]benzenemethanol (14b): a solution of aldehyde **13b** (0.5mmol) in CH$_2$Cl$_2$ (3 mL) was slowly dropped into a suspension of NaBH$_4$ (20 mg, 0.5 mmol) in EtOH (2 mL). The solution was stirred at room temperature for 2h, then poured into brine (10 mL) and extracted with CH$_2$Cl$_2$ (3x10 mL). The organic phase was dried (Na$_2$SO$_4$), and the solvent evaporated under vacuum. The crude alcohol **14b** was obtained in quantitative yield as pale-yellow oil and used without any further purification. ^{1}H-NMR(300MHz, CDCl$_3$): δ, ppm = 0.91-0.93 (d, 12H, J= 6.6 Hz); 0.97-0.99 (d, 6H, J=6.4 Hz); 1.05-1.22 (m, 12H); 1.35-1.39 (m, 8H); 3.99 (t, 4H, J= 3.8); 4.48 (bs, 2H); 6.81-6.84 (m, 4H); 6.95-6.97 (d, 2H, J= 8.3); 7.03-7.05 (m, 4H); 7.17-7.19 (d, 2H, J= 8.3). ^{13}C-NMR (75 MHz, CDCl$_3$): 19.67, 22.59, 22.68, 24.63, 27.94, 29.84, 36.30, 37.29, 39.23, 66.65, 71.83, 115.23, 120.70, 126.02, 126.30, 128.12, 128.91, 130.28, 140.93, 140.93, 148.37, 155.27. HRSM (EI) (m/z): [M]$^+$ found 587.4342; molecular formula C$_{39}$H$_{57}$NO$_3$ requires 587.4338.

4-[bis[4-(2-cyclohexylethoxy)phenyl]amino]benzenemethanol (14c): it was obtained as pale yellow oil in nearly quantitative yield, following the same procedure of **13b**, and used without any further purification. ^{1}H-NMR(300MHz, CDCl3): δ, ppm = 0.92-1.02 (m, 4H); 1.18-1.28 (m, 6H); 1.46-1.52 (m, 2H); 1.57-1.78 (m, 15H); 3.95 (t, 4H, J= 6.7 Hz); 4,57 (bs, 2H); 6.77-6.82 (m, 4H); 6.89-6.92 (d, 2H, *J*= 8.3 Hz); 6.99-7.03 (m, 4H); 7.14-7.17 (d, 2H, *J*= 8.3 Hz). ^{13}C-NMR (75 MHz, CDCl$_3$): δ, ppm = 26.16, 26.47, 33.24, 33.47, 36.66, 64.93, 66.11, 76.57, 77.00, 77.42, 115.17, 120.64, 120.64, 126.27, 128.04, 132.76, 140.76, 148.37, 155.26. HRSM (EI) (m/z): [M]$^+$ found 525.3368; molecular formula $C_{35}H_{45}NO_3$ requires 527.3399.

4,8-bis(3,7-dimethyloctyl)benzo[1,2-*b*:4,5-b']dithiophene (16): A mixture of magnesium turnings (0. 27 g, 11.2 mmol) and a few crystals of I_2 in dry THF (3 mL); was heated to reflux under argon atmosphere, then a solution of 3,7-dimethyloctyl bromide (2.3 g, 11.2 mmol) in dry THF (6 mL) was slowly added. The mixture was heated 1h under stirring then cooled to room temperature and diluted with THF (6 mL), then solid 4,8-dehydrobenzo[1,2-b:4,5-b']dithiophene-4,8-dione **13** (0.34 mg, 1.6 mmol) was added in one portion. The reaction was refluxed under stirring for 9h, then cooled to room temperature and treated with a solution of $SnCl_2.2H_2O$ (1.64 g, 7.3 mmol) in 1 M HCl (10 mL,) then heated to reflux for 3.5 h. After evaporation of the solvent the mixture was taken up with H_2O (15 mL) and CH_2Cl_2 (30 mL), filtered over a pad of celite then extracted with CH_2Cl_2 (3x10 mL). The organic phase was dried over Na_2SO_4 and the solvent evaporated. The crude product was purified by column chromatography (eluent: hexane) to give **14** as a colourless oil in 51% yield. ^{1}H-NMR (300 MHz, CDCl$_3$): δ, ppm = 0.88-0.90 (d, 12H, J=6.0 Hz); 1.05-1.07 (d, 6H, J=6.0 Hz); 1.16-1.66 (m, 18H); 1.72-1.83 (m, 2H); 3.09-3.27 (m, 4H); 7.46 (bs, 4H). ^{13}C-NMR (75 MHz, CDCl$_3$): δ, ppm = 19.19, 20.40, 24.20, 27.47, 30.54, 32.73, 36.15, 38.83, 121.20, 125.33, 128.67, 135.25, 137.20. HRMS-EI (m/z): [M]$^+$ found 470.3024; molecular formula $C_{30}H_{46}S_2$ requires 470.3041.

2.5. DSSC Preparation DSSCs have been prepared adapting a procedure reported in the literature. [24] In order to exclude metal contamination all of the containers were in glass or Teflon and were treated with EtOH and 10% HCl prior to use. Plastic spatulas and tweezers have been used throughout the procedure. FTO glass plates were cleaned in a detergent solution for 15 min using an ultrasonic bath, rinsed with pure water and EtOH. After treatment in a UV-O3 system for 18 min, the FTO plates were treated with a freshly prepared 40 mM aqueous solution of $TiCl_4$ for 30 min at 70 °C and then rinsed with water and EtOH. A transparent layer of 0.20 cm^2 was screen-printed using a 20-nm transparent TiO2 paste (Solaronix T/SP). The coated transparent film was dried at 125 °C for 6 min and then another layer was screen-printed by using a light scattering TiO_2 paste with particles > 100 nm (Solaronix R-SP). The coated films were thermally treated at 125 °C for 6 min, 325 °C for 10 min, 450 °C for 15 min, and 500 °C for 15 min. The heating ramp rate was 5 - 10 °C/min. The sintered layer was treated again with 40 mM aqueous $TiCl_4$ (70 °C for 30 min), rinsed with EtOH and heated at 500 °C for 30 min. After cooling down to 80 °C the TiO_2 coated plate was immersed into a 0.5 mM solution of the dye for 20 h at room temperature in the dark. Counter electrodes were prepared according to the following procedure: a 1-mm hole was made in a FTO plate, using diamond drill bits. The electrodes were then cleaned with a detergent solution for 15 min using an ultrasonic bath, 10% HCl, and finally acetone for 15 min using an ultrasonic bath. After thermal treatment at 500 °C for 30 min, a 15 μL of a 5 x 10-3 M solution of H_2PtCl_6 in EtOH was added and the thermal treatment at 500 °C for 30 min repeated. The dye adsorbed TiO_2 electrode and Pt-counter electrode were assembled into a sealed sandwich-type cell by heating with a hot-melt ionomer-class resin (Surlyn 30-μm thickness) as a spacer between the electrodes. A drop of the electrolyte solution was added to the hole and introduced inside the cell by vacuum

---

[24][] Ito, S.; Murakami, T. N.; Comte, P.; Liska, P.; Grätzel, C.; Nazeeruddin, M. K.; Grätzel, M., Fabrication of thin film dye sensitized solar cells with solar to electric power conversion efficiency over 10%. *Thin Solid Films* 2008, 516: 4613-4619.

backfilling. Finally, the hole was sealed with a sheet of Surlyn and a cover glass. A reflective foil at the back side of the counter electrode was taped to reflect unabsorbed light back to the photoanode.
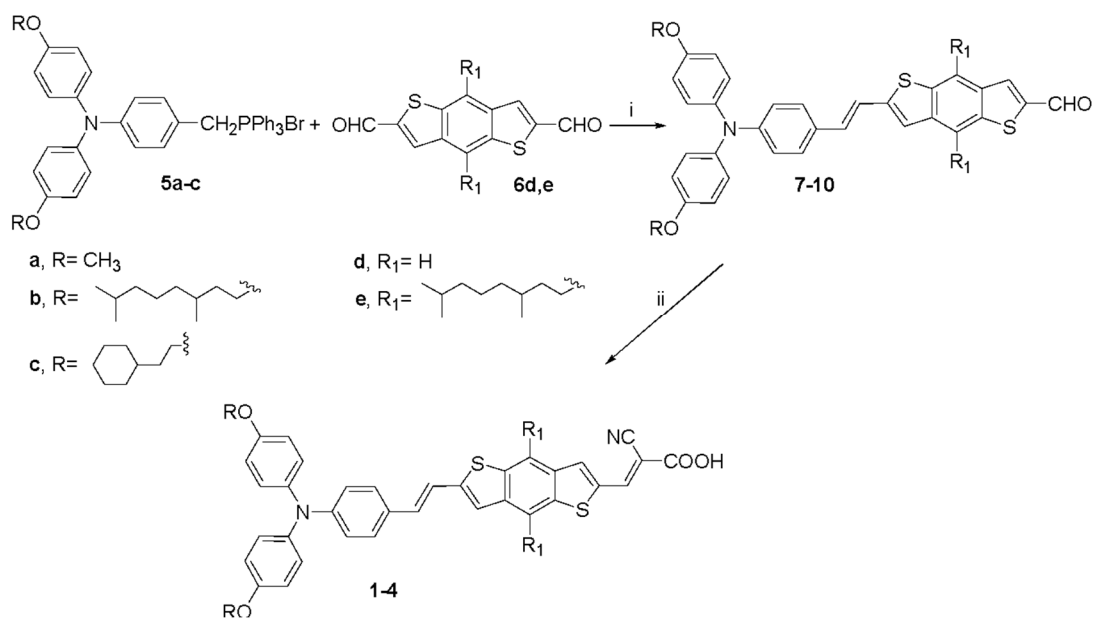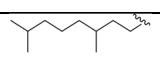
3. Results and discussion
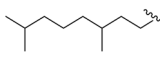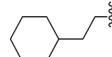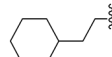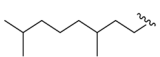
3.1 Synthesis

The synthesis of new dyes **1**– **4** was accomplished following the general synthetic route depicted in scheme 1. The first step is a Wittigreaction between phosphonium salts **5a-c** and BDT_1 di-aldehydes **6d,e** to give mono-formyl derivatives **7**– **10**, which in turn were condensed with the cyanoacetic acid to give dyes **1**– **4** in good yields.

More in detail, the Wittig reaction of phosphonium salts **5b,c** and bis-aldehydes **6d,e** was run in DMF at room temperature under phase transfer catalysis with 18-crown-6 ether and K_2CO_3 as a base, and gave formyl derivatives **7**– **10** in rather good yields

The last synthetic step was the condensation of aldehydes **7**– **10** with cyanoacetic acid, with the catalysis of piperidine, in refluxing THF, to give crude dyes **1**– **4**, that were first purified by column chromatography on silica gel, then treated with a HCl (0.5 N) solution, filtered and obtained as dark red solids. The phosphonium salts **5b,c** and dialdehyde **6e**, not previously reported in the literature, were prepared as described below in Scheme 2, while **5a** and **6d,e** were previously reported. [13] In particular, the synthesis of **5b** and **5c** was carried out starting from 4,4'-dihydroxytriphenylamine **11**, [17] was alkylated with the appropriate alkylbromide, in the presence of K_2CO_3 as a base and 18-crown-6 in refluxing CH_3CN, to give the corresponding alkoxy substituted triarylamines **12b,c**.

Scheme 1: i) K₂CO₃, DMF, 18-crown-6, r.t. 12h; ii) CNCH₂CO₂H, piperidine, THF 67 °C, 8h.

The subsequent formylation of **12b, c** with the Vilsmeier salt gave aldehydes **13b, c** in good yields. The reduction of the formyl group with NaBH₄ gave, in quantitative yields, the corresponding alcohols **14b, c** which, by treatment with PPh₃ hydrobromide in refluxing CHCl₃, gave phosphonium salts **5b, c** in rather good yields.

17
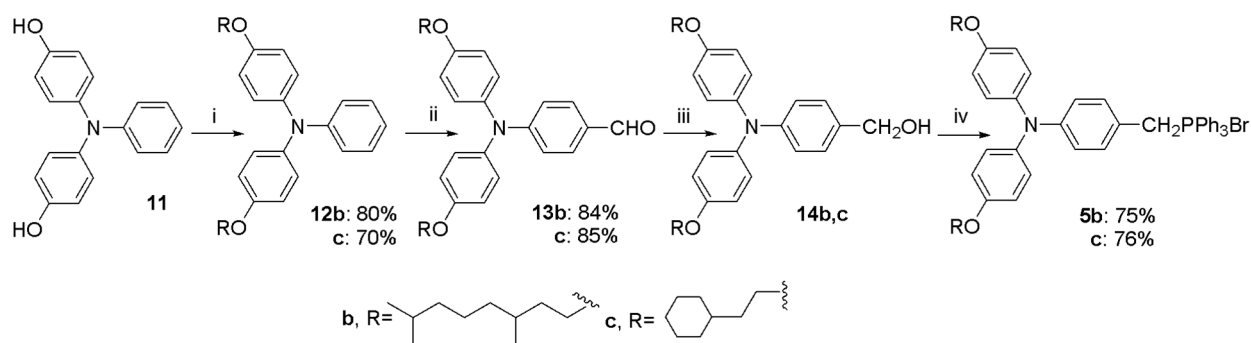
Scheme 2: i) R-Br, K$_2$CO$_3$, 18-crown-6, CH$_3$CN, 80 °C 10 h; ii) ClCH=NMe$_2$Cl, dichloroethane, 80 °C 6h. iii) NaBH$_4$, MeOH r.t. 4h iv) PPh$_3$HBr, CHCl$_3$, 62 °C 5 h.

Benzodithiophene bis-aldehyde **6d** was prepared as already reported [13] while the new 3,7-dimethyloctyl disubstituted BDT$_1$ bis-aldehyde **6e** was synthesized starting from benzo[1,2-b:4,5-b']dithiophene-4,8-dione **15** (Scheme 3)**,** which was reacted with 3,7-dimethyloctylmagnesium bromide, heating in THF solution followed by the addition of tin(II) chloride, that gave 4,8-bis-(3,7-dimethyloctyl)benzodithiophene **16** in 51% overall yield. This was treated with 3 equivalents of butyllithium, followed by the addition of DMF to give the new bis-aldehyde **6e** in 80% yield.
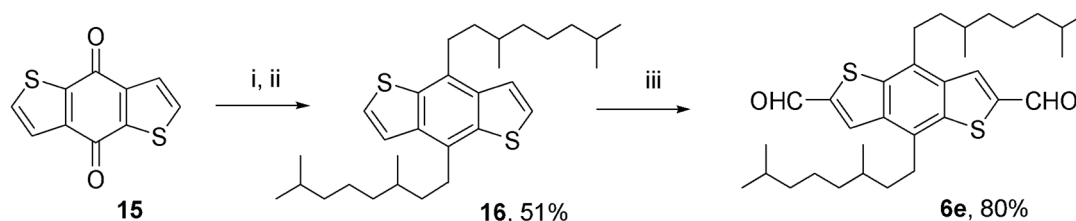
Scheme 3: i) 3,7-dimethyloctylmagnesium bromide, THF, 67 °C, 9h; ii) SnCl$_2$, HCl 1M, 67 °C, 4h; iii) BuLi, THF, -78 0 °C , DMF, 3h.

The new chromophores **1-4** were completely characterized and, as a complement to the experimental work, their molecular and electronic structures and the exciton energies were investigated by means of DFT/TDDFT calculations. Moreover, the optical and redox properties as well as DSSC performances of dyes **1-4** and their dependence on the nature and position of the alkyl chains were investigated.

3.2 Theoretical calculations

First, the geometry optimization of the new compounds *in vacuo* was performed. All the molecules have been simulated in their protonated form, and are characterized by donor-acceptor planar geometries (from the nitrogen lone pair to the cyanoacrylic acid group), except for the two *O*-alkyl substituted phenyl rings in the donor part of the structures, as previously observed for the reference **CR29** dye. (Figure 3) The presence of lateral alkyl chains on BDT_1 spacer (dye **1** and **4)** causes a consistent steric hindrance near the molecule, but does not modify the structure geometry. This arrangement suggests a strong conjugation between the donor, the BDT_1 spacer and cyanoacrylic anchoring group as confirmed by the observation of the electronic structure of the sensitizers.
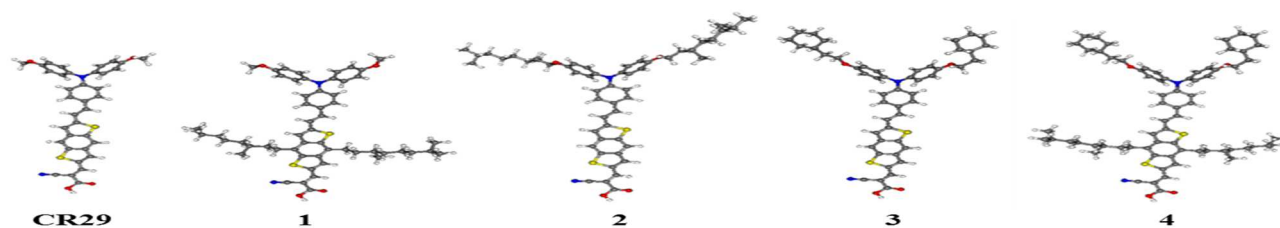
Figure 3. Optimized geometries of the investigated dyes **CR29** and **1-4** .

All the investigated dyes exhibit a strong push-pull behavior, characteristic for these D-π-A compounds in which the HOMO is mainly localized on the triphenylamine donor moiety, and the LUMO extends over the π-bridge and the acceptor cyanoacrylic acid with the largest component localized on the latter. (Figure 4)
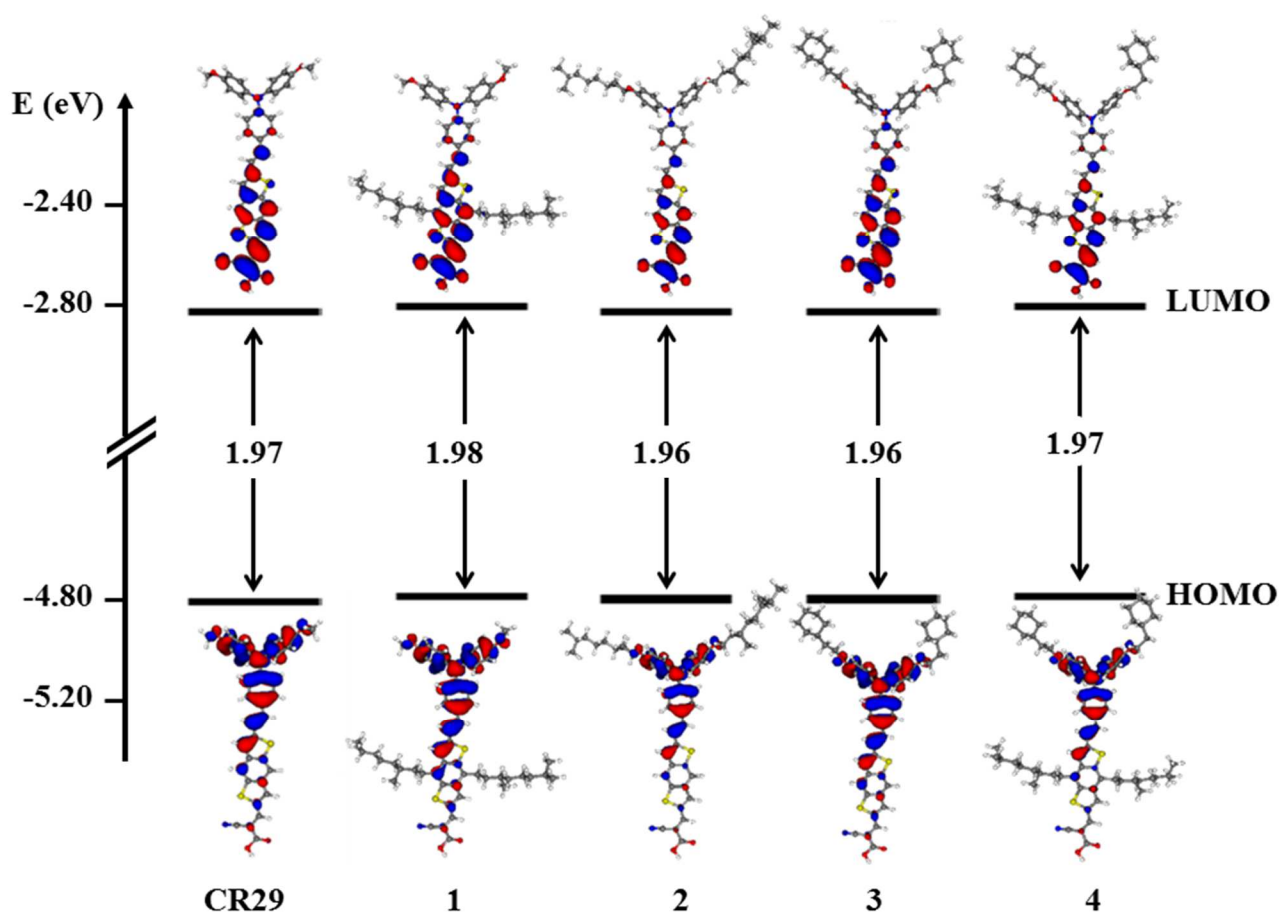
Figure 4. HOMO-LUMO energy levels and isodensity plots for the considered dyes.

The calculated HOMO and LUMO energy levels are in quite good agreement with their experimental analogues, obtained by electrochemical characterization discussed in the next paragraph (see Table 2). The energy gaps are comprised in a 0.02 eV range, between 1.96 eV and 1.98 eV. The slight differences among the dyes are due to the fact that the dye backbone structure is essentially the same along all the series, while the alkoxyl substituents little affect the electronic properties of the sensitizers. On the other hand, it is expected that the bulky chains on the BDT spacer on dyes **1** and **4** will probably have a stronger effect on the packing of the dye upon adsorption on the TiO_2 surface and thus on the interfacial properties.

3.3. UV-Vis characterization

A study of the absorption profile of dyes 1–4 in different solvents were carried out: normalized

UV-Vis spectra in solvents with increasing polarity namely: dichloromethane (DCM),

tetrahydrofuran (THF), EtOH and acetonitrile (ACN) are reported in figures 5–8. (see also SI) All

the dyes display broad absorptions covering a wide wavelength range in the visible region and

exhibit two prominent absorption peaks. (Table 1)

Table 1. Uv-Vis λ_{max} absorption of dyes **CR29** and 1–4 in solvents with increasing polarity and ε_r.

Solvent[a]	CR29	1	2	3	4
	λ_{max} nm ($\varepsilon \cdot \cdot 10^3$ M^{-1}cm^{-1})				
DCM	368 (27.1)	384 (40.0)	376 (32.3)	371 (30.7)	384 (34.7)
	459 (34.8)	489 (59.8)	488 (34.9)	469 (32.0)	491 (46.1)
THF	375 (29.6)	377 (31.6)	373 (30.2)	371 (39.7)	378 (32.0)
	477 (37.1)	499 (51.7)	486 (51.8)	476 (68.6)	487 (44.5)
EtOH	368 (24.3)[b]	370 (23.8)	371 (23.8)	363 (28.7)[b]	369 (35.6)[b]
	453 (33.4)[b]	468 (50.1)	454 (24.8)	454 (41.5)[b]	465 (46.0)[b]
ACN	379 (28.6)[b]	370 (21.0)	359 (22.1)[b]	346 (25.2)[b]	363 (24.8)[b]
	476 (40.5)[b]	459 (34.7)	430 (31.0)[b]	436 (38.1)[b]	472 (44.1)[b]

[a] [C] $\approx 2 \cdot 10^{-5}$ M [b] Traces of TFA were added to solubilise the dye.

TDDFT calculations well reproduced the features of the absorption spectra despite a slight shift

toward lower energies (see supporting information for a detailed list of the calculated transitions)

and allowed us to gain information regarding the character of the electronic transitions. The

absorption bands in the shorter wavelength region (<400 nm) originate from the $\pi-\pi^*$ electronic

excitations, and involves HOMO, HOMO-1, LUMO and LUMO+1 molecular orbitals, essentially

localized within the triarylamine donor and π-bridge segments. The main bands in the visible

region, having higher extinction coefficients, correspond to the intramolecular charge transfer (ICT)

transition from triarylamine donor (HOMO) to the cyanoacrylic acid acceptor (LUMO), and are mainly influenced by the solvent polarity. [13,25] In fact, as known for many push-pull dyes, this absorption band is slightly blue-shifted in polar solvents (EtOH, ACN) with respect to that in DCM as expected for a polarized structure, which is preferentially solvated by polar solvents. In addition dyes 1– 4 bear a carboxylic group, whose ionization equilibrium is known to be affected by solvent parameters [26] e.g. acid/base properties, solvating ability and relative permittivity (ε_r). For acids with a comparable pKa, as can be assumed for 1– 4, an increase in ε_r of the solvent (from DCM to ACN) increases the ionization, shifting acid/base equilibrium toward the deprotonated form of the dye, in which a reduced donor-acceptor interaction causes a blue shift in absorption. This hypothesis was further confirmed by the addition of triethylamine (TEA) or trifluoroacetic acid (TFA) to the dye solutions that respectively caused a hypsochromic or bathochromic effect in UV absorption. (See SI)
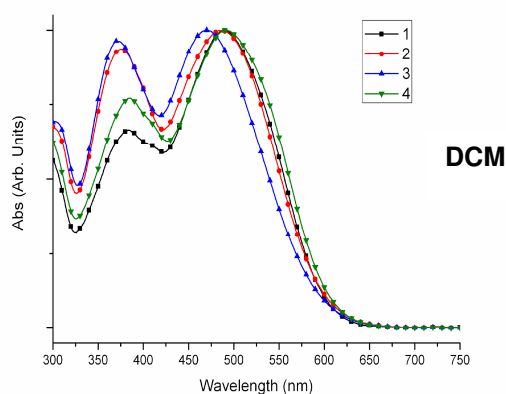
Figure 5. Dyes **1-4**: absorption spectra in DCM
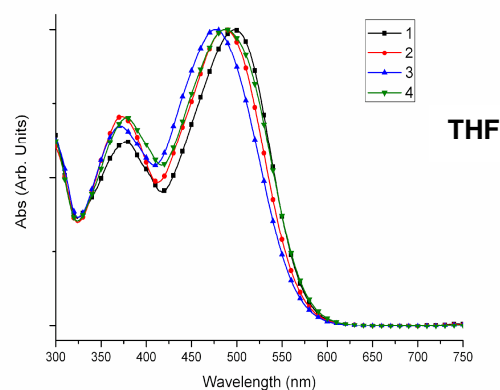
Figure 7. Dyes **1-4**: absorption spectra in THF

[25] Shen P., Liu Y., Huang X., Zhao B., Xiang N., Fei J., Liu L., Wang X., Huang H., Tan S. Efficient triphenylamine dyes for solar cells: Effects of alkyl-substituents and π-conjugated thiophene unit *Dyes and Pigm.*2009 83:187–197.

[26] Reichardt C. Solvent Effects on Homogeneous Chemical Equilibria . In *Solvents and Solvent Effects in Organic Chemistry*, IV Ed.2010, p. 107-163.Wiley-VCH Verlag GmbH & Co. KGaA Weinheim.
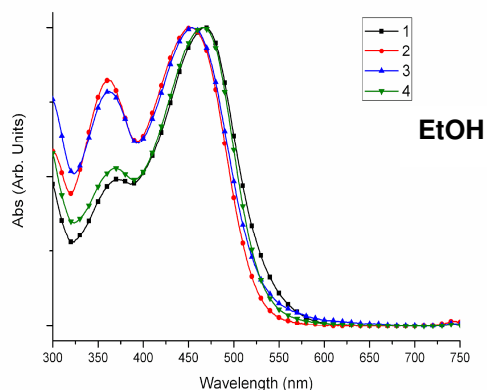
Figure 6. Dyes **1-4**: absorption spectra in EtOH   Figure 8. Dyes **1-4**: absorption spectra in ACN.
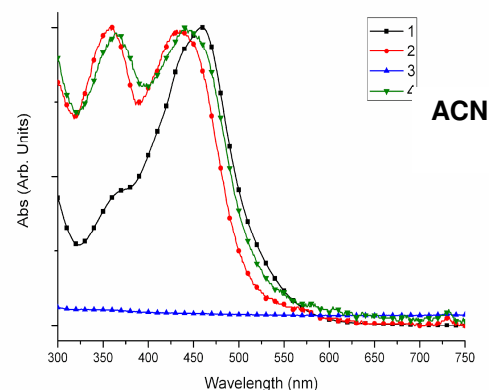
Moreover, considering the influence of alkyl substituents on dye optical properties, as expected, the absorption wavelengths (λ_{max}) of dyes increase as the alkyl chain is longer and in particular 3,7-dimethyloctyl group appears as the best substituent both when inserted on BDT$_1$ spacer (dye **1)**, and on triarylamine unit (dye **2**). The effect of cyclohexylethyl as substituent of triarylamine unit is comparable to that of OCH$_3$. The presence of both alkyl chains, as in dye **4,** doesn't make any significant improvement of dye optical features, thus dye **1** can be considered as the best molecule in term of light absorption.

3.4. Electrochemical properties

The investigation of the redox properties of the four new chromophores **1-4** was carried out by cyclic voltammetry, taking as comparison parent chromophore **CR29 [**13] and selected building blocks **17**, **18** and **19**, whose CV patterns are shown in Figure 9 (see also SI). Table 2 collects peak potentials and related energy parameters HOMO and LUMO and energy gap (E_g), calculated from the equations (1-3) reported in the SI [27,28] ultimately based on the absolute value for the normal hydrogen electrode (NHE).[29] For sake of comparison theoretical HOMO, LUMO and E_g are also

[27][] Ashraf R. S., Shahid M., Klemm E., Al-Ibrahim M., Sensfuss S., *Macromol. Rapid Commun.* **2006**, *27:* 1454–1459.

[28][] Wong W.-Y., Wang X.-Z., He Z., Djurisic A. B., Yip C.-T., Cheung K.-Y., Wang H., Mak C. S. K., Chan W.-K., *Nat. Mater*. 2007, 6: 6521–527.

[29][] Trasatti S., The absolute electrode potential: an explanatory note. *Pure Appl. Chem*. 1986, 58: 955–966.

reported in table 2. First of all, it is interesting to compare the redox properties of parent dye **CR29** with **1 (SB19)**, in which the di-alkyl substitution on the BDT_1 ring is the only modification. The discussion is also supported by the comparison of their building blocks **17**, **18** and **19**.
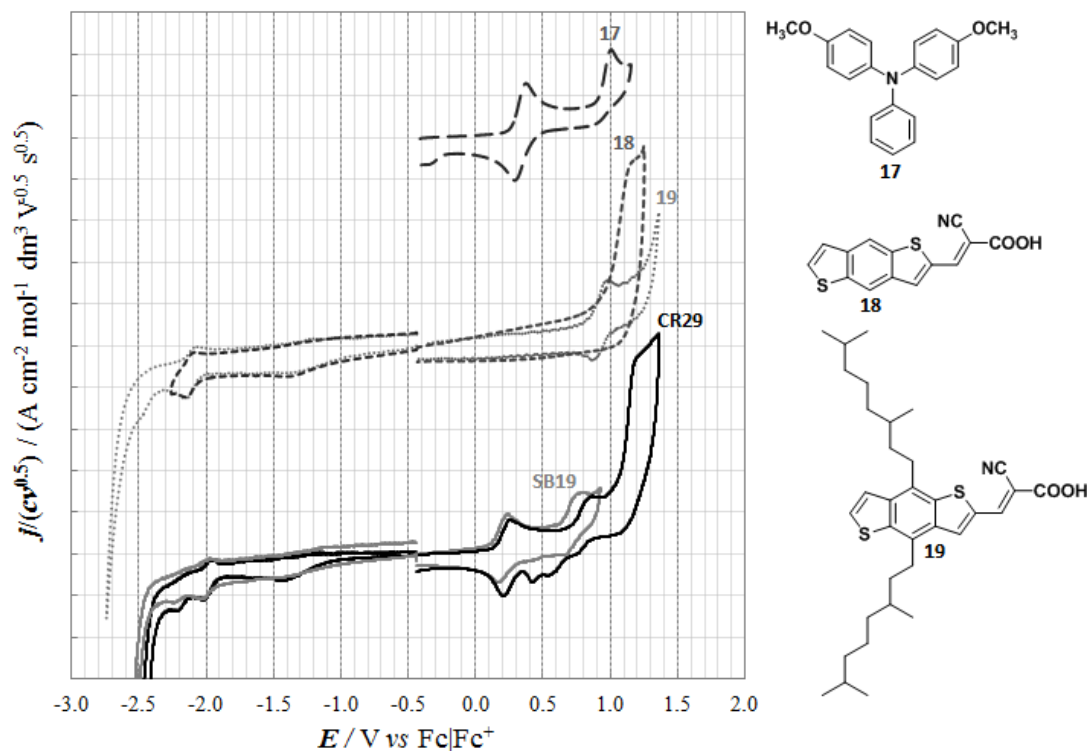
Figure 9. CV patterns comparison of dyes **CR29**, **SB19 (1)** and their precursors **17**, **18** and **19** in CH_2Cl_2 + 0.1 M TBAP at 0.2 V s^{-1}

Comparing the CV patterns of building blocks **17** and **18** with that of dye **CR29** resulting from their combination (Figure 9, Table 2), the first oxidation, chemically and electrochemically reversible, is predominantly localized on the amino terminal group and the first reduction, also chemically and electrochemically reversible, on the cyanoacrilic one, consistently with the theoretical HOMO and LUMO computations in the precedent paragraph 2.2 and as already discussed in our former paper. [13] In dye **CR29,** consistent with the larger LUMO and HOMO delocalization (Figure 4), both the first reduction and the first oxidation peak are shifted to potentials significantly more favourable

than in the separated building blocks **17** and **18** (first oxidation: from 0.38 to 0.26 V; first reduction: from -2.15 to -1.98 V).

Table 2. Peak potentials, related energy parameters, LUMO, HOMO, experimental and theoretic Eg.

| Dye | $E_{p,cI}$ | $E_{p,cII}$ | $E_{p,aI}$ | $E_{p,aII}$ | LUMO | | HOMO | | E_g | |
	V(Fc$^+$|Fc)				Exp. (eV)	Theo. (eV)	Exp. (eV)	Theo. (eV)	Exp. (eV)	Theo. (eV)
17			0.38	1.01			-5.18			
18	-2.15		1.15		-2.65		-5.95		3.30	
19	-2.15	-2.49	0.98		-2.65		-5.78		3.13	
CR29	-1.98	-2.21	0.26	0.86	-2.82	-2.84	-5.06	-4.81	2.24	1.97
1	-1.99	-2.23	0.24	0.76	-2.81	-2.81	-5.04	-4.79	2.23	1.98
3	-2.06	-2.25	0.29	0.88	-2.74	-2.84	-5.09	-4.80	2.35	1.96
4	-2.05	-2.26	0.25	0.78	-2.75	-2.81	-5.05	-4.78	2.30	1.97
2	-2.03	-2.27	0.23	0.80	-2.77	-2.84	-5.03	-4.80	2.26	1.96

[a] CH$_2$Cl$_2$ + 0.1 M TBAP, at potential scan rates typically ranging from 0.05 to 2 V s^{-1}.

Interestingly, in building block **19**, the dialkylation of the benzene ring in the BDT$_1$ unit leaves the reduction peak unchanged with respect to **18** (-2.15 V in both compounds), while resulting in a significant positive shift of the oxidation one (from 1.15 to 0.98 V), consistent to the ~ 50 mV positive shift per alkyl substituent typically observed in organic solvent for model aromatic systems such as ferrocene. [30] These values are consistent with the reduction being predominantly localized on the cyanoacrylic group and the oxidation on the BDT unit, and with the rapidly decreasing of inductive effects with increasing distance.

Comparing **CR29** with **SB19** in the same Figure 9 affords to evaluate the effect of the BDT$_1$ dialkylation within the entire chromophore. Consistent with the previous discussion, both the first

[30][] Noviandri I., Brown K. N., Fleming D. S., Gulyas P.T., Lay P.A., A. F. Masters, L. Phillips, the decamethyl ferrocenium/decamethylferrocene redox couple: a superior redox standard to the ferrocenium/ferrocene redox couple for studying solvent effects on the thermodynamics of electron transfer J. Phys. Chem. B, 1999, 103: 6713-6722.

reduction (from -2.21 to -2.23V) and the first oxidation (from 0.26 to 0.24 V), mostly localized on the terminal sites, appear nearly unaffected (Table 2). Instead, the second oxidation process is clearly shifted at a less positive potential (from 0.86 to 0.76) by 100 mV; the same is also observed for dialkylated chromophore **4** with respect to its parent **3** (from 0.88 to 0.78). It is worthwhile to observe that the negative shift of the BDT-localized oxidation, as a consequence of the inductive effect of the two alkyl chains, results for the BDT_1-cyanoacrylic fragment of all dyes in an oxidation potential comparable to that of the second oxidation of the amino fragment **17**, so that in principle there could be uncertainty as to the site concerned by the second oxidation: the amino or the dialkylated-BDT_1 one. However, on account of their reciprocal conjugation, it is probable that the second oxidation globally involves the main conjugated backbone thus concurrently affecting both the amino and the BDT_1 site.

Concerning the energy parameters, since the first reduction is practically unaffected by the alkyl presence (-1.99 V in **1** vs 1.98 V in **CR29**; -2.05 V in **4** vs -2.06 V in **3**) and the first oxidation only slightly affected (0.24 V in **1** vs 0.26 V in **CR29**; 0.25 V in **4** vs 0.29 V in **3**), the alkylation of BDT_1 unit leaves the LUMOs practically constant, while the HOMOs are slightly higher and the energy gaps slightly decrease This small effect is not observed in the computation results, which however do not take into account the creation of net charges in the polar (solvent+supporting electrolyte) medium.

The effect of increasing the bulkiness of the *O*-alkyl chains on the amino site can be instead evaluated comparing dye **CR29** and **1** bearing *O*-Me substituent to **2** (*O*-3,7-dimethyloctyl), **3** and **4** (*O*-2-cyclohexylethyl). Surprisingly, in all cases the most conspicuous effect is the negative shift of both the reduction peaks. (Table 2) Moreover, the twin reduction peak couple possibly appears less and less evident, with the first peak becoming prominent with respect to the second one and even of comparable height with respect to the first oxidation one (especially in **4**). These features are indeed intriguing, since bulky substituents on the amino site appear to mostly affect the redox properties of the opposite terminal group. So far it can only be observed that such an effect should be more of

thermodynamic than of kinetic nature, since, in spite of the neat shift of the peak potential, the electron transfer appears kinetically facile also with the bulkier substituents (the observed $E_{p,Ic}$ remaining nearly invariant with increasing scan rate). In any case, as a consequence of this effect the insertion of long O-alkyl chains on the amino terminal results in significant LUMO rising (at constant HOMO) and significantly larger gap, quite unlike alkylation on the BDT_1 ring, which, as discussed above, results in a slight HOMO rising (at constant LUMO) and slightly narrower gap.

3.5 Photovoltaic performance of the dyes

The four new dyes have been used as sensitizers in liquid DSSCs. Solar devices were prepared using a double layer film consisting of a transparent 20-nm particles layer (10 μm) of anatase TiO_2 and a scattering layer (5 μm) containing optically dispersing anatase > 100 nm particles. The liquid electrolytes Z960 and A6986 were used for testing the photovoltaic properties of devices. In addition, we have investigated the photovoltaic response of the devices by varying the amount of chenodeoxycholic acid (CDCA) as a de-aggregating co-adsorbent agent [31] in the sensitizer solution (CDCA:dye = 0:1, 1:1, and 30:1) finding that the best performances were reached using a relative concentration of 1:1 for **1** and 30:1 in the case of **2** , **3** , **4**.

The measured photovoltaic performances under AM 1.5 solar standard conditions and double-layer TiO_2 films with a 30:1 CDCA:dye ratio are listed in Table 3 (see SI for photovoltaic measurements with different CDCA:dye ratios). The properties were recorded at different irradiance intensities (1 sun = 1000 W m^{-2}) and compared to those of benchmark dye N719 measured under the same fabrication conditions. The overall power conversion efficiencies PCE were derived from the equation: PCE = J_{sc} x V_{oc} x FF, where J_{sc} is the short circuit current density, V_{oc} the open circuit

---

[31] [] T. Marinado, M. Hahlin, X. Jiang, M. Quintana, E. M. J. Johansson, E. Gabrielsson, S. Plogmaker, D. P. Hagberg, G. Boschloo, S. M. Zakeeruddin, M. Grätzel, H. Siegbahn, L. Sun, A. Hagfeldt, H. Rensmo, *J. Phys. Chem. C* **2010**, *114*, 11903-11910.

voltage, and FF the fill factor. Figure 10A shows the photocurrent-voltage curves of DSSCs based

on the new dyes (see SI for the photocurrent-voltage curves at different irradiation intensities).

Table 3. Detailed photovoltaic parameters of the devices made with the dyes **1**-**4** and with 30:1 CDCA:dye ratio at different light intensities

Device[a]	Irradiance [sun]	J_{sc} [mA cm^{-2}]		V_{oc} [mV]		FF [%]		PCE [%]	
1 [b]	1	11.2	(14.0)	738	(748)	72	(70)	6.0	(7.3)
	0.8	9.0	(11.0)	729	(738)	73	(71)	6.0	(7.3)
	0.5	6.3	(8.0)	717	(728)	73	(72)	6.6	(8.4)
	0.2	2.7	(3.4)	691	(701)	75	(73)	6.0	(7.6)
2 [b]	1	8.8	(11.2)	664	(680)	73	(74)	4.3	(5.6)
	0.8	6.6	(8.7)	661	(672)	76	(75)	4.2	(5.5)
	0.5	4.6	(6.2)	649	(662)	77	(76)	4.6	(6.2)
	0.2	2.0	(2.6)	627	(638)	78	(77)	5.0	(6.5)
3 [b]	1	10.7	(13.9)	671	(684)	73	(71)	5.3	(6.8)
	0.8	8.4	(11.1)	659	(674)	74	(72)	5.2	(6.8)
	0.5	6.0	(7.8)	648	(662)	75	(74)	5.8	(7.7)
	0.2	2.5	(3.2)	620	(632)	76	(76)	5.1	(6.6)
4 [b]	1	6.5	(7.8)	657	(668)	76	(76)	3.2	(3.9)
	0.8	5.0	(6.1)	646	(658)	76	(76)	3.1	(3.8)
	0.5	3.4	(4.2)	635	(646)	76	(76)	3.3	(4.1)
	0.2	1.5	(1.7)	612	(620)	76	(77)	3.4	(4.1)
N719[c]	1	15.6	(17.9)	720	(722)	72	(71)	8.1	(9.2)

[a] Incident intensity of AM1.5 solar light; values without mask are in brackets; double TiO$_2$ layer (10+5 μm). [b] Dye solution of 2 x 10^{-4} M in EtOH, electrolyte A6986 (1.0 M dimethyl imidazolium iodide, 0.03 M I2, 0.05 M LiI, 0.1 M guanidinium thiocyanate and 0.5 M 4-t-butylpyridine in acetonitrile/valeronitrile 85/15).[32] [Dye solution of 2 x 10^{-4} M in EtOH/THF 1:1electrolyte Z960 (1.0 M dimethyl imidazolium iodide, 0.03 M I2, 0.05 M LiI, 0.1 M guanidinium thiocyanate and 0.5 M 4-t-butylpyridine in acetonitrile/valeronitrile 85/15)[33].[c] Dye solution of 5 x 10^{-4} M in EtOH solution with 1:1 CDCA; electrolyte A6141 (0.6 M *N*-butyl-N-methyl imidazolium iodide, 0.03 M I$_2$, 0.10 M guanidinium thiocyanate, and 0.5 M 4-*t*-butylpyridine in acetonitrile/valeronitrile 85:15).

The best PCE was recorded for **1**, where notable values of 6.6 and 8.4% (with and without a black tape shading mask, 0.40 mm^2, on top of devices mask, respectively) were measured at 0.5 sun irradiation. It is worth noting that dye **1** is the molecule with the simplest donor core, where methoxy substituents are present on the triphenylamine scaffold. The long alkyl chains on the BDT$_1$

[32][] Bessho T. , Zakeeruddin S.M., Yeh C.-Y., Diau E. W.-G., Grätzel M., Highly Efficient Mesoscopic Dye-Sensitized Solar Cells Based on Donor–Acceptor-Substituted Porphyrins *Angew. Chem. Int. Ed.* 2010, *49*: 6646-6649.

[33][] Abbotto A., Barolo C., Bellotto L., De Angelis F., Gratzel M., Manfredi N., Marinzi C., Fantacci S., Yum J.-H., Nazeeruddin M. K., Electron-rich heteroaromatic conjugated bipyridine based ruthenium sensitizer for efficient dye-sensitized solar cells. *Chem. Comm.* 2008, 5318-5320.

spacer are likely responsible for a minimized interaction TiO$_2$-electrolyte and, thus, decreased charge recombination from the semiconductor oxide to the oxidized form of the electrolyte. This is confirmed by the highest measured photovoltage, being the only dye of the series with values > 0.7 V. Though molecule **4** has the same substituted pattern on the spacer, much lower PCE were recorded. In this case the lowest efficiency originates from the lower photocurrent. Once more, sensitizer **1** is the best system of the investigated series, with photocurrent reaching values over 11 mA cm^{-2} in presence of a device mask.

To gain further insights incident monochromatic photon-to-current conversion efficiencies (IPCE) were investigated (Figure 10B). The shape of these spectra follows those of the corresponding absorption spectra. The photocurrent values calculated by integrating the IPCE spectra and using the AM 1.5G spectrum nicely matched those measured with masked solar cells. [34] IPCE peaks

---

[34][] S. Ito, M. K. Nazeeruddin, P. Liska, P. Comte, R. Charvet, P. Pechy, M. Jirousek, A. Kay, S. M. Zakeeruddin, M. Gratzel, Photovoltaic characterization of dye-sensitized solar cells: effect of device masking on conversion efficiency. *Prog Photovoltaics* 2006, *14*: 589-601.

Supporting Information

Benzodithiophene Based Organic Dyes for DSSC: Effect of Alkyl Chain Substitution on dye efficiency

Clara Baldoli,[a*] Stefania Bertuolo,[b] Emanuela Licandro,[b] Lucia Viglianti,[b] Patrizia Mussini[b], Gabriele Marotta,[c] Paolo Salvatori,[c, d] Filippo De Angelis,[c] Paola Manca,[e] Norberto Manfredi,[e] Alessandro Abbotto[e*]

Synthesis of compound **18** and **19**

Absorption spectra of **1** in different solvents

Fig. S1

Absorption spectra of **2** in different solvents

Fig. S2

Materials and reagents :Silica gel 60 (70–230 mesh, Merck) was used for column chromatography. ^{1}H NMR spectra were acquired with a Bruker ADVANCE DRX-400, a Bruker AC300, or an AMX 300 MHz spectrometer; chemical shifts (δ) are reported in parts per million relative to the solvent residual peak ([D6]acetone, [D6]DMSO, CDCl3). IR spectra were recorded with a Fourier Bruker Vector 22 FT; UV spectra were recorded with a Jasco V-520 or Agilent 8453 UV/Vis spectrophotometer in a range of λ from 190 to 800 nm at room temperature. HRMS spectra were recorded with a Bruker Daltonics ICR-FTMS APEX II. Melting points were obtained with a Büchi B-540 melting point apparatus and are uncorrected. HPLC analyses were performed with an Agilent 1100 series equipped with a PDA detector and a reverse-phase ZORBAX Eclipse XBD-C18 column (4.6/ 150 mm, 5 μm particle size); samples were analyzed with 1 mL/min acetonitrile/water (80:20) with 0.1% TFA.

Synthesis of 18 and 19

Compounds **18** and **19** were prepared from the corresponding aldehydes **20a**[13] and **20b** using the same experimental conditions for dye **2**.

4,8-bis-(3,7-dimethyloctyl) benzo[1,2-b:4,5-b']dithiophen-2-carboxaldehyde (20b)

n-BuLi (1.6 M in hexane, 1.44 mL, 2.3 mmol) was added to a solution of **16** (2. mmol) at -78 °C in THF (7 mL) and the yellow mixture thus obtained was stirred for 1.5 h at the same temperature. Then DMF (0.5 mL) was added dropwise and the yellow mixture solution was stirred for 2.5 h at -70 °C then allowed to reach room temperature. A saturated solution of NH_4Cl (10 mL) was added and the mixture extracted with CH_2Cl_2 (3x15 mL). The organic phases were washed with H_2O (15 mL), dried (Na_2SO_4), filtered and the solvent was evaporated. The crude product was purified by column chromatography on silica gel (eluent: hexane/AcOEt 95:5) to afford **20b** as a light orange oil (70%). IR (nujol, cm^{-1}): 1672 (νCO). ^{1}H-NMR (300 MHz, CDCl$_3$): δ, ppm = 0.87 (d, J=6.6 Hz, 6H), 0.88 (d, J=6.6 Hz, 6H), 1.06 (d, 6.0 Hz, 3H), 1.06 (d, 6.0 Hz, 3H), 1.40-1.10 (m, 12H), 1.69-1.48 (m, 6H), 1.87-1.71 (m, 2H), 3.25-3.15 (m, 4H), 7.47 (d, J=5.6 Hz, 1H), 7.58 (d, J=5.6 Hz, 1H), 8.17 (s, 1H),

10.14 (s, 1H). ^{13}C-NMR (75 MHz, CDCl$_3$): δ, ppm = 19.63, 22.62, 22.70, 24.72, 28.00, 30.90, 33.26, 36.54, 37.01, 37.13, 39.31, 121.89, 128.64, 129.88, 132.81, 132.94, 134.67, 137.95, 138.94, 139.36, 142.51, 184.61. HRMS-EI+ (m/z): [M]$^+$ calcd. for C$_{31}$H$_{46}$OS$_2$: 498.299010, found: 498.294830. HRSM (EI) (m/z): [M]$^+$ found 498.2948; molecular formula C$_{31}$H$_{46}$OS$_2$ requires 498.2990.

18: orange solid (83%). M.p.: 165-167 ^{1}H-NMR (300 MHz, CDCl$_3$): δ, ppm= 7.56 (d, J=6.1 Hz, 1H), 7.99 (d, J=6.1 Hz, 1H), 8.40 (s, 1H), 8.63 (s, 1H), 8.68 (s, 1H), 8.73 (s, 1H). ^{13}C-NMR (75 MHz, CDCl$_3$): δ, ppm = 99.61, 114.2, 120.89, 123.64, 128.81, 132.84, 134.12, 134.67, 135.76, 138.34, 139.36, 141.51, 148.61, 160.18. HRSM (EI) (m/z): [M]$^+$ found 283.9845; molecular formula C$_{14}$H$_7$NO$_2$S$_2$ requires 283.9846.

19: orange solid (85%). M.p. : 148-150 °C ^{1}H-NMR (300 MHz, CDCl3): δ, ppm = 0.87 (d, 6H, *J*=6.6 Hz), 0.88, (d, 6H, *J*=6.6 Hz), 1.06 (d, 3H, *J*=5.9 Hz), 1.07 (d, 3H, *J*=5.9 Hz), 1.1-1.48 (m, 12H), 1.50-1.71 (m, 6H), 1.72-1.87 (m, 2H), 3.10-3.28 (m, 4H), 7.48 (d, 1H, *J*=5.6 Hz) , 7.61(d, 1H, *J*=5.6 Hz), 8.18 (s, 1H), 8.52 (s, 1H). ^{13}C-NMR (75 MHz, CDCl3): δ, ppm = 19.65, 22.60, 22.68, 24.71, 27.97, 30.85, 31.13, 33.15, 33.27, 36.65, 36.96, 37.05, 37.21, 39.28, 99.31, 114.97, 122.03, 129.35, 129.65, 132.83, 134.19, 134.82, 135.59, 138.32, 139.44, 140.34, 149.23, 166.70. HRSM (EI) (m/z): [M]$^+$ found 565.3104; molecular formula C$_{34}$H$_{47}$NO$_2$S$_2$ requires 565.3048.

UV-vis CH2Cl2 (4.42E-05 M): λmax = 386 nm (ε= 2.85E+04 M-1 cm-1)

UV-Vis spectra of dyes 1-4 in different solvents

Figure S1: Normalized UV-Vis spectra of dyes **1** in different solvents

DYE
Solvent
[2*10^{-5}M]
$\square$ **max**
$\square$ **max Acid**
$\square$ **max Base**
$\square$ $\square$ $\square$ **Acid**
$\square$ $\square$ $\square$ **Base**
1(SB19)
EtOH
468
497
433

29
35

ACN
459
495
462
36
-3

THF
499
499
461
0
38

Toluene
474
515
458
41
16

CH$_2$Cl$_2$
489
522
464
33
25

Figure S2: Normalized UV-Vis spectra of dyes **2** in different solvents

DYE
Solvent
[2*10^{-5}M]
λ**max**
λ**max Acid**
λ**max Base**
$\Delta\lambda$**Acid**
$\Delta\lambda$**Base**
2 (CB2944)

EtOH
474
488
360
14
114

ACN

430
482
447
52
-17
THF
486
487
459
1
27
Toluene
464
505
454
41
10
CH$_2$Cl$_2$
488
510
456
2
32

Figure S3: Normalized UV-Vis spectra of dyes **3** in different solvents

DYE Solvent [2*10^{-5}M]	$\square_{max}$	$\square_{max}$ **Acid**	$\square_{max}$ **Base**	$\square\square\square$**Acid**	$\square\square\square$**Base**
3(CB324)					
EtOH	454	482	426	28	28
ACN[a]	Insol.	481	450	//	//
THF	476	487	451	11	25
Toluene	456	504	454	48	2
CH2Cl2	469	510	460	41	9

-

Figure S4: Normalized UV-Vis spectra of dyes **4** in different solvents

DYE Solvent [2*10^{-5}M]	$\square_{max}$	$\square_{max}$ **Acid**	$\square_{max}$ **Base**	$\square\square\square$**Acid**	$\square\square\square$**Base**
4(CB844)					
EtOH					

465
499
455
34
10
ACN[a]
440
472
463
32
-23
THF
487
499
461
12
26
Toluene
482
514
461
32
21
CH_2Cl_2
491
520
469
29
22

Table S5. Calculated molecular orbitals energy levels (eV) in acetonitrile solution.

CR29
CB324
13SB19
CB844
CB2944
L+3
-0.46
-0.45
-0.36
-0.35
-0.46
L+2
-0.56
-0.54
-0.54
-0.53

-0.55

L+1

-1.63

-1.64

-1.60

-1.61

-1.63

L

-2.84

-2.84

-2.81

-2.81

-2.84

H

-4.81

-4.80

-4.79

-4.78

-4.80

H-1

-5.64

-5.63

-5.53

-5.52

-5.64

H-2

-6.11

-6.11

-6.00

-6.00

-6.11

H-3

-6.28

-6.27

-6.29

-6.26

-6.60

H-L Gap

1.97

1.96

1.98

1.97

1.96

Table S6. Comparison between calculated excitation energies, along with their oscillator strengths and composition, for dyes **1-4** in vacuo and acetonitrile.

MPW1K –Vacuum

State

E (eV)
λ (nm)
ƒ
composition (%)

	(CR29)
	1
	2.61
	476
	1.8645
86 H→L	
	2
	3.24
	382
	0.0997
62 H-1 →L	
30 H-2→L	
	3
	3.52
	353
	0.7060
43 H -2→L	
20 H→L+1	
	4
	3.65
	340
	0.1588
74 H →L+1	
	(CB324)
	1
	2.59
	479
	1.8995
86 H→L	
	2
	3.23
	384
	0.1261
64 H-1 →L	
28 H-2→L	
	3
	3.50
	354
	0.7425
43 H -2→L	
17 H-1→L	
15 H→L+1	
11 H-4→L	
	4
	3.63
	341
	0.1602
73 H →L+1	
11 H-2 →L	
	(13SB19)
	1
	2.60
	477
	1.8283
83 H→L	
10 H-1→L	
	2
	3.10
	399

64 H-1 →L
27 H-2→L

3
3.51
353
0.6150

49 H -2→L
20 H-1→L
10 H-4→L

4
3.64
341
0.2476

80 H →L+1

(CB844)
1
2.58
480
1.8656

84 H→L

2
3.10
400
0.0601

64 H-1 →L
26 H-2→L

3
3.49
355
0.6684

48 H -2→L
20 H-1→L

4
3.62
342
0.2370

78 H →L+1

(CB2944)
1
2.58
480
1.8650

86 H→L

2
3.23
384
0.1285

64 H-1→L
28 H-2→L

3
3.50
354
0.7391

43 H-2→L
17 H-1→L
16 H →L+1

4
3.63

341
0.1423

72 H →L+1

MPW1K –Acetonitrile
CR29
1
2.46
503
2.0001

83 H→L

2
3.14
395
0.1482

67 H-1 →L
23 H-2→L

3
3.45
360
0.6226

49 H -2→L
14 H-4 →L

4
3.55
349
0.2088

75 H →L+1

CB324
1
2.45
505
2.0303

83 H→L
10 H-1→L

2
3.13
396
0.1641

68 H-1 →L
22 H-2→L

3
3.43
361
0.6449

48 H -2→L
14 H-4 →L
13 H→L+1
12 H-1→L

4
3.54
350
0.2077

73 H →L+1
10 H-2 →L

13SB19
1
2.44
507

1.9562

80 H→L
13 H-1→L

2
3.01
412
0.0777

67 H-1 →L
21 H-2→L

3
3.42
362
0.6001

52 H -2→L
14 H-4 →L
14 H-1→L

4
3.54
350
0.2860

79 H →L+1

CB844
1
2.44
509
1.9857

81 H→L

2
3.00
413
0.0786

68 H-1 →L
21 H-2→L

3
3.41
362
0.6242

52 H -2→L
14 H-4 →L
14 H-1→L

4
3.53
351
0.2812

81 H →L+1

CB2944
1
2.46
505
2.0154

83 H→L

2
3.13
396
0.1571

68 H-1→L
23 H-2→L

3
3.44

48 H -2→L
14 H-4 →L
13 H-1→L
13 H →L+1

74 H →L+1

Table S7: Cartesian coordinates of optimized dyes.
Cartesian coordinates of optimized dye 1(SB19)

130

C	4.108093	0.008499	-1.244329
C	4.742285	0.304715	-2.462965
C	5.815938	-0.494180	-2.869609
C	6.266391	-1.553650	-2.078895
C	5.622667	-1.844436	-0.870598
C	4.535486	-1.055798	-0.463759
N	4.280792	1.386029	-3.272753
C	5.182502	2.323678	-3.804038
C	4.923100	2.976667	-5.024621
C	5.819362	3.906719	-5.531438
C	7.020043	4.229702	-4.868440
C	7.267017	3.569926	-3.645414
C	6.376836	2.647190	-3.122974
C	7.922172	5.203160	-5.462902
C	9.141294	5.584662	-5.008653
C	10.010827	6.554822	-5.623233
S	9.565590	7.437563	-7.094141
C	11.109061	8.299962	-7.095784
C	11.915835	7.905977	-5.979973
C	11.257921	6.919801	-5.178307
C	13.193494	8.473938	-5.780961
C	13.597407	9.411762	-6.730402
C	12.789714	9.803900	-7.844150
C	11.505258	9.235349	-8.041844
C	13.446144	10.780711	-8.641377
C	14.703264	11.140301	-8.193366

S	15.142260	10.260406	-6.720925
C	15.514841	12.102446	-8.862890
C	16.766443	12.580170	-8.583317
C	17.551632	12.158245	-7.470667
N	18.193556	11.812478	-6.561937
C	2.884319	1.472427	-3.556763
C	2.172453	0.346789	-3.981755
C	0.799475	0.412525	-4.229097
C	0.120343	1.625839	-4.071237
C	0.830199	2.761828	-3.652327
C	2.189821	2.683193	-3.388069
C	17.324165	13.599902	-9.510009
O	16.749615	14.035291	-10.489258
O	18.562203	14.003738	-9.146171
H	15.065151	12.536542	-9.754170
H	18.835238	14.664312	-9.809415
C	14.084210	8.058797	-4.631512
C	10.613185	9.658133	-9.186739
H	11.695553	6.478768	-4.289842
H	13.015603	11.224671	-9.532379
H	9.545946	5.138691	-4.101678
H	5.594832	4.389117	-6.480212
H	4.017758	2.745127	-5.574957
H	6.592613	2.172167	-2.172053
H	8.165822	3.796872	-3.078973
H	7.554902	5.659099	-6.382809
H	2.695302	-0.595407	-4.114005
H	0.279262	-0.481738	-4.552683
H	3.272262	0.618819	-0.916555
H	4.048774	-1.289597	0.477954
H	6.310225	-0.284235	-3.813292
H	2.726619	3.563833	-3.048838
O	-1.214701	1.807783	-4.291741
H	0.288663	3.693844	-3.524079
O	5.969622	-2.859780	-0.026280
H	7.104362	-2.148464	-2.424135
C	7.060013	-3.690615	-0.390327
H	7.162307	-4.420608	0.414656
H	6.869295	-4.217528	-1.334856
H	7.992543	-3.117540	-0.480265
C	-1.981696	0.692353	-4.715380
H	-3.004877	1.056358	-4.824681
H	-1.630505	0.303438	-5.680529
H	-1.962161	-0.116743	-3.973045
H	11.227370	9.864683	-10.069865
H	9.957574	8.822139	-9.464196
C	9.741031	10.887065	-8.844053
C	8.725318	11.282803	-9.935963
H	9.197322	10.672431	-7.914933
H	10.394497	11.743634	-8.624009

C	7.768334	12.365388	-9.392950
C	9.418753	11.728657	-11.233352
H	8.119422	10.390462	-10.162955
C	6.562365	12.680590	-10.290656
H	7.394067	12.038809	-8.411866
H	8.338247	13.288711	-9.207193
C	5.588032	13.678290	-9.647277
H	6.902412	13.088703	-11.252339
H	6.039794	11.742254	-10.522232
C	4.397701	14.098440	-10.532705
H	5.201620	13.255788	-8.706690
H	6.147909	14.581860	-9.364361
C	3.602569	15.229545	-9.863046
H	4.807631	14.490175	-11.476939
C	3.472267	12.920275	-10.873880
H	2.776948	15.568039	-10.500470
H	3.169992	14.894020	-8.911215
H	4.240107	16.096272	-9.651011
H	2.626339	13.252120	-11.487558
H	3.992879	12.132808	-11.429225
H	3.062284	12.469824	-9.959954
H	8.692666	11.984263	-12.011659
H	10.041126	12.616213	-11.055872
H	10.063873	10.944301	-11.643961
H	14.721565	8.904648	-4.349535
H	13.469360	7.837880	-3.749703
C	14.958802	6.829060	-4.962894
C	15.822722	6.313582	-3.792803
H	14.299962	6.018216	-5.301705
H	15.608796	7.071208	-5.815364
C	16.483027	4.975308	-4.188083
C	16.858132	7.355096	-3.339282
H	15.147517	6.112042	-2.944379
C	17.209873	4.237956	-3.053615
H	15.706128	4.309750	-4.592614
H	17.187065	5.154634	-5.014908
C	17.738079	2.863169	-3.489497
H	18.051524	4.842053	-2.688941
H	16.521804	4.124073	-2.204430
C	18.577763	2.112821	-2.436493
H	16.891650	2.226365	-3.791224
H	18.351834	2.995324	-4.392729
C	19.191686	0.842853	-3.044712
H	19.405353	2.775314	-2.137671
C	17.772585	1.769014	-1.173946
H	19.828474	0.321338	-2.320118
H	18.407834	0.142254	-3.362003
H	19.804473	1.075906	-3.923733
H	18.392525	1.226735	-0.450019
H	17.388689	2.664162	-0.673082

H	16.914385	1.129038	-1.419959
H	17.455006	6.990032	-2.497216
H	17.548308	7.600229	-4.157088
H	16.385460	8.288186	-3.014943

Cartesian coordinates of optimized dye 2(CB2944)

124

C	7.676158	1.728391	1.120926
C	6.661675	1.472685	0.183449
C	6.389597	2.439748	-0.789471
C	7.095079	3.644282	-0.825507
C	8.110098	3.886754	0.108615
C	8.395701	2.914002	1.079383
N	5.943046	0.238198	0.214006
C	6.693033	-0.975221	0.282642
C	6.392269	-1.957354	1.232080
C	7.130248	-3.140751	1.303786
C	8.207489	-3.345621	0.432758
C	8.521905	-2.357306	-0.513123
C	7.770399	-1.193833	-0.592329
O	9.002412	-4.453746	0.420852
C	8.761576	-5.482790	1.381419
O	8.871282	5.017128	0.158460
C	8.629672	6.051456	-0.796211
C	4.539887	0.221455	0.194493
C	3.789575	1.296453	0.711587
C	2.403425	1.267737	0.681936
C	1.686670	0.177132	0.149452
C	2.449525	-0.892539	-0.366805
C	3.833539	-0.874650	-0.349865
C	0.233892	0.208680	0.159042
C	-0.618253	-0.749031	-0.283809
C	-2.056159	-0.681451	-0.256249
C	-2.923021	-1.649731	-0.703084
C	-4.305707	-1.322617	-0.553072
C	-4.484145	-0.030860	0.042106
S	-2.930590	0.724301	0.390135
C	-5.430055	-2.086399	-0.904623
C	-6.689093	-1.554007	-0.658312
C	-6.863961	-0.265132	-0.063952
C	-5.734938	0.502535	0.288765
S	-8.230768	-2.320411	-1.010034
C	-9.106788	-0.919248	-0.362080
C	-8.238927	0.058093	0.087203
C	-10.525300	-0.782223	-0.295745
C	-11.532111	-1.623597	-0.681711
C	-12.926857	-1.155708	-0.462228
O	-13.842968	-2.059150	-0.876027

C	-11.319642	-2.903367	-1.273041
N	-11.144902	-3.948906	-1.756293
O	-13.228846	-0.086645	0.031433
H	6.856387	4.371958	-1.592500
H	8.017138	-0.438898	-1.332471
H	9.357138	-2.530237	-1.184571
H	5.568425	-1.798568	1.921275
H	4.302337	2.149032	1.142864
H	1.851916	2.108545	1.097000
H	1.950455	-1.751724	-0.805982
H	4.386440	-1.708603	-0.768191
H	7.899050	0.985402	1.880513
H	9.182276	3.116504	1.799558
H	5.613824	2.251813	-1.525623
H	6.865611	-3.882306	2.048653
C	9.808582	-6.567385	1.156242
H	8.825250	-5.060779	2.393127
H	7.747271	-5.888897	1.247646
C	9.612141	7.179088	-0.502204
H	8.781407	5.662315	-1.814458
H	7.587511	6.388215	-0.715730
H	-10.872426	0.154260	0.137260
H	-14.714870	-1.663519	-0.691123
H	-5.308712	-3.066556	-1.356320
H	-5.857492	1.482602	0.740762
H	-2.576081	-2.583887	-1.132954
H	-8.593415	0.989584	0.517595
H	-0.195903	1.118803	0.578655
H	-0.225445	-1.672569	-0.705189
C	9.578187	8.335524	-1.522526
H	9.416304	7.564769	0.507566
H	10.618710	6.742574	-0.480082
C	10.752394	9.300988	-1.254041
H	9.731387	7.901968	-2.524237
C	8.223315	9.063547	-1.522044
C	10.968842	10.385078	-2.319973
H	10.607089	9.777614	-0.272479
H	11.675233	8.709249	-1.168181
C	12.225649	11.226968	-2.054041
H	11.039410	9.905301	-3.305900
H	10.097643	11.052717	-2.364347
C	12.453393	12.402104	-3.025984
H	12.167504	11.628348	-1.031444
H	13.111522	10.573003	-2.070891
C	13.630587	13.268658	-2.553894
C	12.675088	11.936585	-4.473277
H	11.547716	13.028862	-3.008141
H	13.777156	14.132955	-3.212462
H	13.468467	13.644767	-1.536648
H	14.564989	12.692078	-2.550530

```
H    8.200676    9.872752   -2.258668
H    7.394554    8.388642   -1.762276
H    8.019387    9.503066   -0.536637
H   12.843759   12.792274   -5.137868
H   13.556169   11.284641   -4.542782
H   11.816582   11.380214   -4.864562
C    9.617759   -7.828834    2.022970
H    9.773172   -6.846375    0.095513
H   10.804494   -6.138850    1.333564
C   10.609080   -8.922930    1.572526
C    9.745026   -7.521307    3.524756
H    8.600054   -8.209806    1.838841
C   10.381100  -10.310194    2.190653
H   10.550353   -9.016347    0.478435
H   11.634677   -8.588941    1.792459
C   11.338727  -11.370718    1.627819
H   10.505719  -10.264043    3.281086
H    9.339757  -10.611801    2.012279
C   11.226331  -12.767958    2.270588
H   11.182239  -11.464065    0.541868
H   12.370854  -11.011750    1.753710
C   12.353785  -13.682043    1.767397
H   11.354202  -12.645384    3.357703
C    9.856698  -13.420369    2.027620
H   12.310974  -14.667773    2.245762
H   12.278664  -13.836331    0.682887
H   13.340784  -13.251066    1.973986
H    9.596831   -8.419005    4.133333
H   10.741380   -7.121928    3.756314
H    9.006364   -6.783826    3.857572
H    9.812086  -14.417088    2.482323
H    9.036290  -12.829780    2.449240
H    9.666438  -13.537915    0.952377
```

**Cartesian coordinates of optimized dye
3 (CB324)**

108

```
S   15.610508   10.301572   -7.036091
C   14.022122    9.553351   -6.967136
C   13.118849   10.144819   -7.904946
C   13.742431   11.183487   -8.646714
C   15.066373   11.403521   -8.316618
C   11.793395    9.671883   -7.994234
C   11.414403    8.639253   -7.157567
C   12.317318    8.045225   -6.215936
C   13.637068    8.515829   -6.127809
C   11.691028    7.001173   -5.468379
C   10.374808    6.777427   -5.793904
```

S	9.826994	7.878527	-7.076749
C	9.508889	5.791635	-5.201077
C	8.213741	5.564017	-5.532604
C	7.310021	4.583257	-4.954892
C	6.006741	4.455094	-5.476402
C	5.099323	3.532754	-4.977394
C	5.452965	2.686503	-3.907507
C	6.752982	2.811824	-3.368866
C	7.651508	3.731179	-3.882805
N	4.544578	1.749785	-3.389249
C	5.005070	0.538830	-2.788413
C	5.951128	-0.273000	-3.438128
C	6.387846	-1.454521	-2.856818
C	5.873865	-1.872585	-1.619025
C	4.919910	-1.078058	-0.971531
C	4.502121	0.120997	-1.552652
C	15.864587	12.402085	-8.949985
C	17.170768	12.763523	-8.766352
C	17.693243	13.868280	-9.614319
O	18.990603	14.145064	-9.355549
C	3.136805	1.982256	-3.452445
C	2.271793	0.985542	-3.934254
C	0.901255	1.197538	-3.976665
C	0.356173	2.420618	-3.555723
C	1.210893	3.423114	-3.080950
C	2.586956	3.193492	-3.020400
C	18.043559	12.148145	-7.821800
N	18.755886	11.644616	-7.049616
O	17.044313	14.464680	-10.451567
H	7.118646	-2.084923	-3.353759
O	6.362505	-3.052620	-1.140941
H	15.348571	12.980477	-9.714316
H	19.236156	14.873208	-9.955906
H	14.331540	8.074114	-5.419261
H	11.099761	10.114105	-8.703564
H	12.204498	6.425968	-4.704645
H	13.235452	11.763905	-9.411381
H	9.982384	5.196395	-4.422452
H	5.707477	5.088866	-6.308340
H	4.111253	3.455862	-5.417532
H	7.045805	2.184280	-2.534282
H	8.635312	3.800355	-3.427347
H	7.775704	6.171301	-6.325300
H	2.684377	0.039949	-4.272164
H	0.228498	0.430431	-4.347341
H	3.769068	0.736932	-1.040788
H	4.505554	-1.371936	-0.014125
H	6.343375	0.031417	-4.403662
H	3.241883	3.970498	-2.637919
O	-1.000141	2.531657	-3.649560

H	0.820927	4.376076	-2.742841
C	5.850726	-3.559521	0.092088
C	-1.622169	3.751792	-3.243890
C	6.547191	-4.888120	0.361226
H	6.053509	-2.844495	0.903696
H	4.761969	-3.680914	0.014265
C	-3.124085	3.611797	-3.463001
H	-1.386477	3.956794	-2.190563
H	-1.227911	4.585033	-3.843385
H	-3.585297	4.582577	-3.229805
H	-3.294201	3.433647	-4.533028
C	-3.814978	2.502077	-2.649050
C	6.165742	-5.543751	1.701069
H	6.326422	-5.575351	-0.466613
H	7.629876	-4.708685	0.337678
C	7.083779	-6.747388	1.995062
H	6.328180	-4.803348	2.502570
C	6.736982	-7.439176	3.321864
H	6.991654	-7.473431	1.172536
H	8.131823	-6.419505	2.002167
C	5.262210	-7.864041	3.366014
H	7.389816	-8.308182	3.473344
H	6.939784	-6.748634	4.154045
C	4.335112	-6.672951	3.084848
H	5.087878	-8.644051	2.610004
H	5.022530	-8.312148	4.338676
C	4.686880	-5.979553	1.758961
H	3.287543	-6.999764	3.068965
H	4.421257	-5.945831	3.906100
H	4.490056	-6.669896	0.923902
H	4.023320	-5.118121	1.610793
C	-5.275918	2.329278	-3.109250
H	-3.284362	1.560850	-2.854436
C	-6.011839	1.234859	-2.321773
H	-5.806711	3.285945	-2.981032
H	-5.301500	2.102910	-4.183711
C	-5.949220	1.491664	-0.809307
H	-7.055452	1.168715	-2.655143
H	-5.551746	0.260173	-2.542191
C	-4.497837	1.656734	-0.336674
H	-6.512785	2.406921	-0.573848
H	-6.437721	0.674860	-0.262673
C	-3.764271	2.751351	-1.128750
H	-4.469090	1.887488	0.735984
H	-3.965566	0.702507	-0.464426
H	-4.226962	3.727249	-0.911260
H	-2.724522	2.815294	-0.783681

Cartesian coordinates of optimized dye 4 (CB844)

```
S   -3.418494    2.529741    -0.833786
C   -3.559546    2.279070    -2.572955
C   -4.914027    2.028366    -2.958831
C   -5.785984    2.055628    -1.836704
C   -5.163288    2.308079    -0.628805
C   -5.247791    1.796595    -4.317865
C   -4.187397    1.834225    -5.212685
C   -2.829956    2.081679    -4.828558
C   -2.497713    2.316193    -3.475958
S   -4.313480    1.582782    -6.958031
C   -2.565726    1.797226    -7.159257
C   -1.950341    2.048011    -5.957071
C   -1.918568    1.707305    -8.442986
C   -2.529479    1.464241    -9.628903
C   -1.910801    1.354648    -10.940124
C   -2.724722    1.141811    -12.071124
C   -2.197869    1.028265    -13.349091
C   -0.807506    1.112175    -13.560993
C    0.019885    1.320977    -12.435519
C   -0.520667    1.441569    -11.166373
N   -0.256320    0.991028    -14.847346
C    0.970130    1.645362    -15.176695
C    1.145246    3.015842    -14.918155
C    2.332964    3.651944    -15.249061
C    3.373190    2.941139    -15.868536
C    3.203283    1.578286    -16.141227
C    2.012313    0.941013    -15.786616
O    4.492522    3.662878    -16.160753
C    5.590479    3.006149    -16.795548
C    6.677093    4.052511    -17.013522
C    7.999194    3.494272    -17.570054
C    9.087697    4.586456    -17.559234
C   10.430544    4.082407    -18.108052
C   10.275033    3.490185    -19.516142
C    9.201326    2.392902    -19.539541
C    7.859089    2.898931    -18.986485
C   -6.674424    1.564243    -4.760103
C   -7.437590    2.878394    -5.040470
C   -8.854588    2.691916    -5.621521
C   -9.782057    1.944186    -4.649921
C   -5.872769    2.371255     0.606068
C   -5.442563    2.601155     1.884813
C   -6.472445    2.597162     2.956526
O   -5.944399    2.832020     4.178993
C   -0.900407    0.212453    -15.855475
C   -1.066278    0.726888    -17.152671
C   -1.666512   -0.034099    -18.145467
```

```
C   -2.138193   -1.325922   -17.865966
C   -1.987664   -1.843677   -16.573704
C   -1.359806   -1.081178   -15.586508
O   -2.720030   -1.986490   -18.908675
C   -3.238105   -3.299048   -18.688898
C   -3.808184   -3.809354   -20.007107
C   -2.791719   -3.960668   -21.154183
C   -1.711895   -5.021408   -20.862355
C   -0.732277   -5.188850   -22.035503
C   -1.465820   -5.512359   -23.344533
C   -2.540536   -4.458939   -23.650278
C   -3.515022   -4.291632   -22.474192
C   -4.082181    2.839390    2.238385
N   -2.970432    3.033374    2.527874
O   -7.659885    2.406483    2.776840
C   -9.435393    4.062161   -6.031494
C   -10.728417   4.004679   -6.858883
C   -11.205548   5.394706   -7.304734
C   -12.539908   5.418404   -8.077164
H   -13.295100   4.915379   -7.452855
C   -13.006255   6.865043   -8.299981
H    2.474411    4.709977   -15.051642
H   -6.945918    2.208189    0.523308
H   -6.692679    2.808905    4.803764
C   -1.072085    2.551780   -3.030143
H   -0.879150    2.201515   -5.888503
H   -6.857223    1.896489   -1.897706
H   -0.840632    1.855308   -8.408095
H   -3.802801    1.078629   -11.940008
H   -2.860504    0.878415   -14.194371
H    1.094810    1.376606   -12.568403
H    0.156410    1.587594   -10.329491
H   -3.611782    1.331664    -9.626987
H   -0.715070    1.729158   -17.377332
H   -1.794702    0.358624   -19.149381
H    1.889236   -0.117725   -15.993490
H    3.989283    1.001760   -16.615125
H    0.341357    3.578306   -14.452984
H   -1.232026   -1.497095   -14.591799
H   -2.337057   -2.839436   -16.326723
H    5.958583    2.190570   -16.154779
H    5.256457    2.565413   -17.744354
H   -2.440726   -3.956613   -18.316541
H   -4.025646   -3.261670   -17.922269
H   -4.287314   -4.779102   -19.808357
H   -4.606963   -3.123840   -20.319584
H    6.288399    4.830635   -17.684205
H    6.867130    4.539464   -16.048276
H    8.336549    2.685748   -16.899772
H    8.742967    5.436215   -18.168509
```

H	9.216313	4.969995	-16.538295
H	11.163538	4.899091	-18.115643
H	10.830682	3.311185	-17.433186
H	9.990057	4.290194	-20.215624
H	11.234032	3.091867	-19.871138
H	9.065611	2.012864	-20.560110
H	9.542404	1.540522	-18.933190
H	7.458375	3.674451	-19.657661
H	7.129418	2.079082	-18.990607
H	-2.287578	-2.991380	-21.280287
H	-4.087827	-5.223425	-22.344129
H	-4.248917	-3.506714	-22.701453
H	-3.092010	-4.727971	-24.560320
H	-2.053004	-3.494245	-23.854680
H	-1.941933	-6.500523	-23.257663
H	-0.751825	-5.581520	-24.175174
H	-0.000933	-5.973689	-21.803492
H	-0.160342	-4.257761	-22.161854
H	-2.204190	-5.986291	-20.661804
H	-1.151453	-4.762670	-19.955075
H	-6.676441	0.948326	-5.669226
H	-7.200028	0.977940	-3.998707
H	-7.497410	3.465554	-4.112647
H	-6.842929	3.477653	-5.742009
H	-8.759583	2.084824	-6.536486
H	-9.606462	4.664560	-5.126151
H	-8.675449	4.602647	-6.614232
H	-10.558028	3.365629	-7.736050
H	-11.528832	3.524646	-6.279176
H	-11.307934	6.031241	-6.413512
H	-10.426805	5.866304	-7.924126
C	-12.460382	4.668285	-9.415717
H	-13.973509	6.896279	-8.815701
H	-13.114537	7.402139	-7.350094
H	-12.284887	7.419065	-8.915043
H	-10.783468	1.810265	-5.071273
H	-9.401639	0.946273	-4.406314
H	-9.890178	2.501323	-3.709331
H	-13.416699	4.719255	-9.949726
H	-11.693877	5.111151	-10.065798
H	-12.213927	3.609479	-9.282681
H	-1.077294	3.199805	-2.146053
C	-0.316629	1.240454	-2.719288
H	-0.529694	3.106409	-3.806298
C	1.170753	1.419343	-2.350147
H	-0.832456	0.714733	-1.903581
H	-0.388168	0.585370	-3.598015
C	1.847897	0.035463	-2.254840
H	1.654543	1.969469	-3.174397
C	1.350180	2.238289	-1.061736

C	3.376314	0.054828	-2.103370
H	1.406495	-0.520814	-1.413798
H	1.597223	-0.537775	-3.159803
C	3.987397	-1.354005	-2.130122
H	3.806534	0.666867	-2.908313
H	3.656941	0.544362	-1.160939
C	5.505338	-1.419932	-1.868696
H	3.478115	-1.969775	-1.374206
H	3.771002	-1.827887	-3.100430
C	5.965623	-2.879490	-1.735329
C	6.322959	-0.695991	-2.949473
H	5.698765	-0.918646	-0.907254
H	7.036574	-2.940252	-1.507440
H	5.422312	-3.399312	-0.937114
H	5.793728	-3.431585	-2.668862
H	2.408227	2.372297	-0.814477
H	0.912428	3.238430	-1.147272
H	0.868842	1.737578	-0.211530
H	7.397279	-0.768580	-2.742016
H	6.145549	-1.142766	-3.937111
H	6.071345	0.367932	-3.014312

Photovoltaics: The following materials were purchased from commercial suppliers: FTO-coated glass plates (2.2 mm thick; sheet resistance ~7 ohm/ square; Solaronix); TiO$_2$ (Solaronix T/SP and R/SP); N719 (Sigma-Aldrich). The thickness of the layers was measured by means of a VEECO Dektak 8 Stylus Profiler. Photovoltaic measurements of DSSCs were carried out with an antireflective layer and with or without black mask on top of the photoanode of 0.38 cm^2 surface area under a 500 W Xenon light source. The power of the simulated light was calibrated to AM 1.5 (100 mW cm^{-2}) using a reference Si cell photodiode equipped with an IR-cutoff filter (KG-5) to reduce the mismatch in the region of 350-750 nm between the simulated light and the AM 1.5 spectrum. Values were recorded after 3 and 24 h, 3 and 6 days of ageing in the dark. *I–V* curves were obtained by applying an external bias to the cell and measuring the generated photocurrent with a Keithley digital source meter. IPCE were recorded as a function of excitation wavelength by using a monochromator with single grating in Czerny-Turner optical design, in AC mode with a chopping frequency of 1 Hz and a bias of blue light (0.3 sun). Absorption spectra were recorded on a V-570 Jasco spectrophotomer.

Table S10. Photovoltaic performances of DSSC using solutions of dyes 2 and 4 in EtOH at different CDCA:dye ratios

Device[a]	CDCA:dye	J_{sc} [mA cm^{-2}]	V_{oc} [mV]	FF [%]	PCE [%]
2[b]	0:1	1.09	642	59	0.4
	1:1	1.13	617	55	0.4
	30:1	12.6	693	73	6.4
4[b]	0:1				

0.09
364
58
0.02
1:1
0.7
524
57
0.2
30:1
7.8
673
73
3.8

[a] Incident intensity of AM1.5 solar light; double TiO_2 layer (10+5 μm). [b] Dye solution of 2×10^{-4} M in EtOH; electrolyte Z960.

Fig. S11: *J/V* curve of DSSC of dyes **1-4** at different light intensities.

Electrochemical measurements. The working electrode was a glassy carbon GC disk embedded Teflon®(Metrohm, 0.033 cm²) or (Amel, 0.071 cm²). The optimized polishing procedure involved surface treatment with a synthetic diamond powder of 1 mm diameter (Aldrich) on a DP-Nap wet cloth (Struers). The operating reference electrode was an aqueous saturated calomel one (SCE), inserted in a compartment filled with the same CH_2Cl_2 + 0.1 M $TBAPF_6$ working medium and ending in a porous frit, preventing significant leakage of water and KCl into the working solution. The experimental peak potentials have been afterwards normalized *vs*. the potential of $Fc^+|Fc$ redox couple (the intersolvental redox potential reference currently recommended by IUPAC), measured in the same conditions. The counter electrode was a platinum disk or wire, embedded in glass.

The ohmic potential drop was compensated for by the positive feedback technique.

Fig S12: Equations 1-3 for the evaluation of HOMO and LUMO levels from CV data

$$.E_{HOMO} / eV = -1e^- \times [E_{pIa} / V \ (Fc^+|Fc) + 4.8 \ V \ (Fc^+|Fc \ vs \ zero)] \quad (1)$$

$$E_{LUMO} / eV = -1e^- \times [E_{pIc} / V \ (Fc^+|Fc) + 4.8 \ V \ (Fc^+|Fc \ vs \ zero)] \quad (2)$$

$$E_g \,/\mathrm{eV} = E_{\mathrm{LUMO}} \,/\, \mathrm{eV} - E_{\mathrm{HOMO}} \,/\, \mathrm{eV} \qquad (3)$$

Fig. S13: A synopsis of CV patterns for the dyes: CR29 and 1-4 at 0.2 V s⁻¹.

Figure S14

Figure S15

$$E_g \,/\mathrm{eV} = E_{\mathrm{LUMO}} \,/\, \mathrm{eV} - E_{\mathrm{HOMO}} \,/\, \mathrm{eV} \qquad (3)$$

ranged from 60% for **4** to 70% for **1**. In order to elucidate the different IPCE responses we separately examined the two components according to eq. (1):

$$IPCE(\lambda) = LHE(\lambda) \times APCE(\lambda) \qquad (1)$$

where LHE is the light-harvesting efficiency, associated to the ability of the cell of harvesting the light, and APCE the absorbed monochromatic photon-to-current conversion efficiency (APCE), that is the internal quantum efficiency associated to the ability of the cell of generating electric current. LHE and APCE characteristics are shown in Figures 10C and 10D, respectively.

The best LHE profile, which directly originates from the absorption spectra as films, was recorded for dye **1** and is in agreement with the higher measured photocurrent. The APCE of **1** is greater than 80% for a broad spectral region spanning from 400 to 550 nm. $APCE_{max}$ reached values greater than 80% for **3** as well but for a less extended wavelength range.

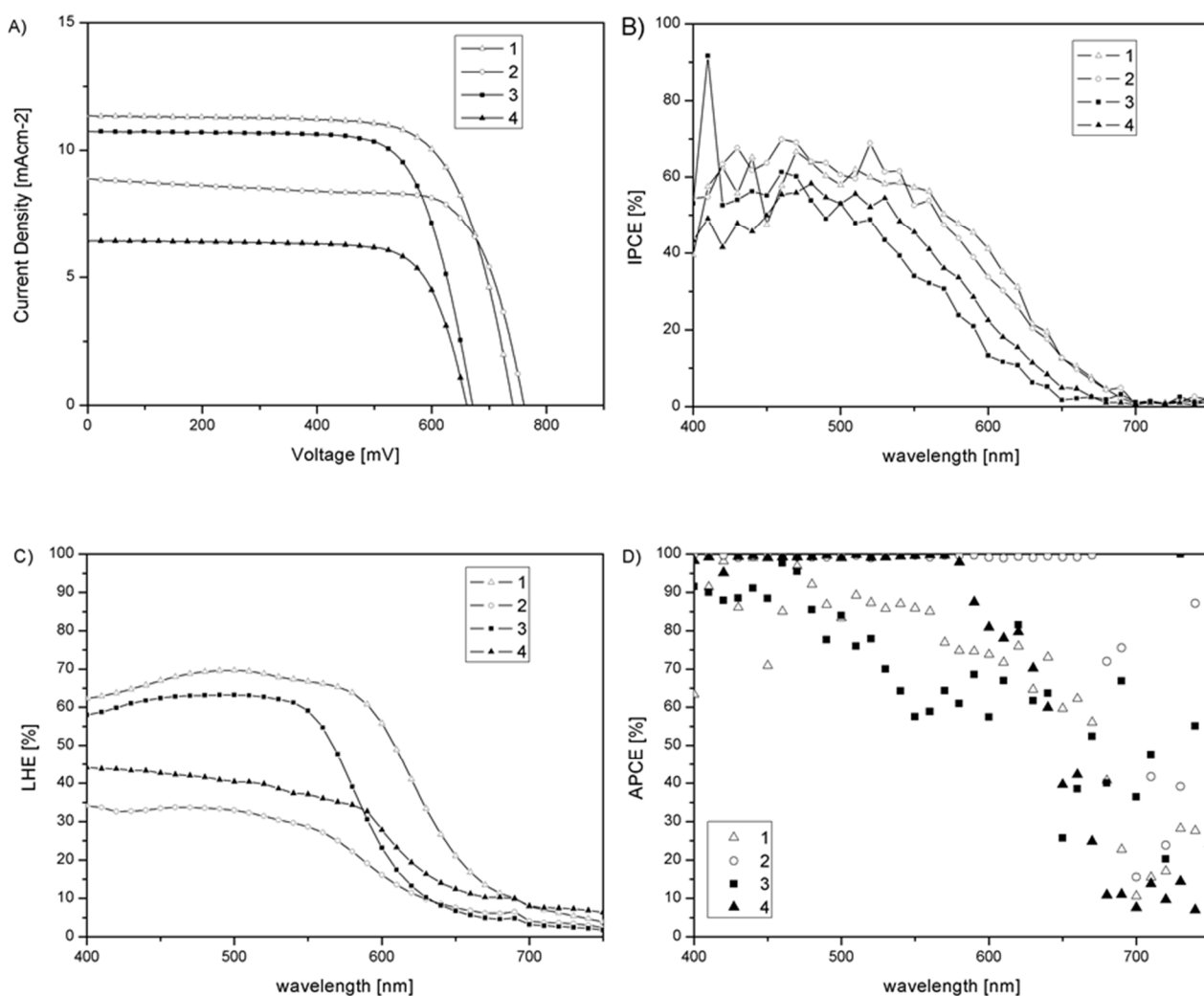**Figure S16**

Figure S17

Figure 10. (A) Comparison of the *J-V* curves of dyes sensitized solar cells under full AM 1.5 solar intensity. (B) Corresponding IPCE. (C) LHE obtained using a 10-μm transparent TiO$_2$ film. (D) APCE obtained from IPCE and LHE.

Therefore we can conclude that the highest photovoltaic response, and thus the overall efficiency, of

1 originates both from an efficient and broad light harvesting and from an improved ability to

convert photons to electrons. In the case of **3** the lower IPCE is either due to a decreased ability to

harvest light over a broad range or to a lower internal quantum efficiency.

The protonation equilibria COOH/ COO$^-$ of the dyes greatly affected the optical properties and the

corresponding photovoltaic characteristics. In particular, we observed, for **2** and **4**, that when

devices were prepared using a EtOH solution of the dyes, where the protonation equilibra are

shifted towards the deprotonated carboxylate form, photocurrents were vey low and PCE close to 0% (see SI). From the previous detailed investigation of the dependence of the dye protonation equilibrium from the solvent nature (paragraph 3.3, fig. 5-7), we identified THF as the best solvent where the protonated COOH form is predominant and thus used EtOH/THF 1:1 solutions of the dyes to sensitize the photoanodes. In this case much higher photocurrents, and efficiencies, were obtained. It is then clear that the equilibrium between the deprotonated COO$^-$ and protonated COOH is critical to afford higher cell efficiencies. The use of 30:1 CDCA:dye EtOH solutions clearly support this hypothesis. In fact, in this case the presence of a larger molar amount of CDCA is enough to shift the equilibrium towards COOH even in the ethanolic solution, whereas the presence of higher CDCA:dye ratios in the EtOH:THF solution afforded similar photocurrents and PCE. To the best of our knowledge this is the first time where the nature of the solvent used for the dye-sensitization bath is clearly found to be critical for reaching much higher efficiencies.

4. Conclusions

We synthesized a series of triarylamine push-pull dyes containing the benzo[1,2-*b*:4,5-*b'*]dithiophene spacer in which bulky alkyl chains were inserted on the triarylamine moiety or on the π-conjugated spacer. The effect of the alkyl chain position on the dye properties and photovoltaic performances were investigated. Electrochemical experiments showed that while alkylation on the BDT_1 ring only results in a slight HOMO rising (at constant LUMO) and a slightly narrower gap, the insertion of long O-alkyl chains on the amino terminal results in significant LUMO rising (at constant HOMO) and significantly larger gap.

The new dyes were used as sensitizers in liquid DSSC. The best PCE was recorded for dye **1** (6.6% at 0.5 sun, 8.4% without mask on top of the cell), the molecule with the simplest donor core, to be compared with a value of 8.1% for N719-based devices under the same fabrication conditions. Therefore the photovoltaic performance of the sensitizer **1** was only ~20% less than the benchmark dye N719. The best LHE profile, in agreement with optical properties, and the APCE values, greater than 80%, suggested that the efficiency of **1** originates from high light harvesting and charge

formation and collection efficiency. Photovoltaic performances were dramatically dependent on the choice of the solvent used for the dye-sensitizing bath. The results were correlated, through extensive optical studies in different solvents and acid/base additives, with protonation equilibria of COOH/COO⁻ group of dyes. These data clearly show that when an unsuitable, though very common, solvent as EtOH is used for dye solutions, misleading PCEs even close to 0% may be obtained, although in the presence of performing sensitizers, as ascertained when proper conditions are alternatively selected, thus showing the strategic importance of selecting appropriate solvents for DSSC fabrication conditions.

References